University of Louisville

ThinkIR: The University of Louisville's Institutional Repository

Electronic Theses and Dissertations

5-2004

Cephalogram pseudo-color and emboss enhancements : anatomical landmark clarity in photostimuable phosphor cephalometrics.

Ryan B. Wiesemann 1977-
University of Louisville

Follow this and additional works at: https://ir.library.louisville.edu/etd

CEPHALOGRAM PSEUDO-COLOR AND EMBOSS ENHANCEMENTS: ANATOMICAL LANDMARK CLARITY IN PHOTOSTIMUABLE PHOSPHOR CEPHALOMETRICS

By

Ryan B. Wiesemann
University of Louisville School of Dentistry

A Thesis
Submitted to the Faculty of
the Graduate School of the University of Louisville
in Partial Fulfillment of the Requirements
for the Degree of

Master of Science

Program in Oral Biology
School of Dentistry
University of Louisville
Louisville, Kentucky

May 2004

Cephalogram Pseudo-Color and Emboss Enhancements: Anatomical Landmark Clarity in Photostimuable Phosphor Cephalometrics

By

Ryan Wiesemann
University of Louisville School of Dentistry

A Thesis Approved on
April 7, 2004

By the following Reading Committee:

_____
Allan G. Farman, PhD, DSc

_____
Baxter E. Johnson, DDS

_____
Anibal Silveira, DDS

_____
James P. Scheetz, PhD

This Thesis is dedicated to my father Dr. Richard J. Wiesemann. Thank you for

being the perfect example as a radiologist, husband, and father. I am only as

strong and successful as the support from my family. Thank you Richard,

Rosemary, Ranney, and Regan.

ACKNOWLEDGEMENTS

ABSTRACT

Post-processing Contrast Enhancement in 8-bit and 16-bit

Photostimuable Phosphor Cephalograms

Ryan Wiesemann

April 7, 2004

Purpose: To evaluate baseline and 3 different image enhancements for the detection of landmarks and overall perceived quality in photostimuable phosphor cephalograms.

Methods: DenOptix images of 48 patients (plus 12 repeats) were presented randomly to 10 observers who rated 11 anatomic landmarks and overall appearance (1 = poor; 2 = satisfactory; 3 = excellent). Equal numbers of 16-bit images with single peak (SP) 16-bit double peak (DP) histograms and 8-bit images were included. Enhancements used were: (1) emboss; (2) pseudocolor; and (3) emboss-pseudocolor. The Friedman Test with Wilcoxon post hoc analysis was applied.

Results and Conclusion: The results support the use of emboss and color enhancements to aid in the quality of landmark identification and improved perception of image quality for photostimuable phosphor cephalograms. Emboss enhancement seems to be best utilized for hard tissue landmarks while color enhancement seems to be best utilized for soft-tissue landmarks.

Key words: Radiology; Cephalometrics; Digital image processing; Orthodontics; Photostimulable phosphor

TABLE OF CONTENTS

LIST OF TABLES

LIST OF FIGURES

Chapter I

Literature Review

During the 1920's the ability to measure craniomaxillofacial structures using
anthropometric techniques created a stir in the orthodontic community.[1] Craniometry, the
science of determining morphology and growth changes on dried skulls using cross-
sectional techniques, was exposing the weaknesses of cephalometry, the science of using
living individuals for studying growth of the head. Cephalometry was orthodontics main
form of study at the time and presented several inadequacies. Then most orthodontists
used measurements based on the interrelations of strictly teeth and jaws, not to mention
only being able to compare patients to benchmark individuals instead of observing the
continuous progression of a single individual. Craniometry's ability to precisely measure
and repeat these measurements confirmed the obsoleteness of orthodontist's usual dental
and facial deformity measurements.[1] In 1922 Paccini first attempted to gain more
information using lateral head radiographs. Then in 1931 Broadbent of the United States
and Hofrath of Germany almost simultaneously developed the cephalostat (Figures 1 and
2).

Figure 1: Broadbent-Bolton (USA) cephalostat
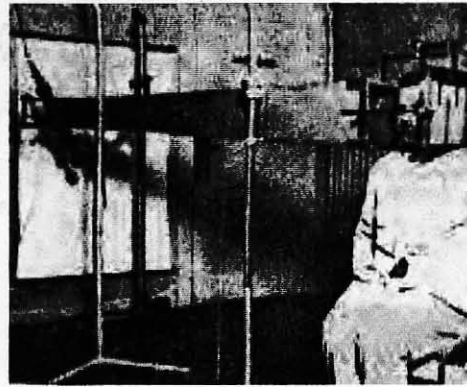
Figure 2: Hofrath (Germany) cephalostat

On February 4, 1931 Broadbent presented to the Chicago Dental Society an instrument and technique that would revolutionize standardized cephalometry becoming a mainstay used even today. He entitled his creation the "head holder" which became better known as the cephalostat. By using this cephalostat and a standardized radiographic technique it was made possible to make accurate determinations of changes in the living head that may be a result of developmental growth or orthodontic treatment.[1] His technique unveiled a way to measure and study the same individual.[1] More

Figure 3: Bolton Room at Case Western Reserve University
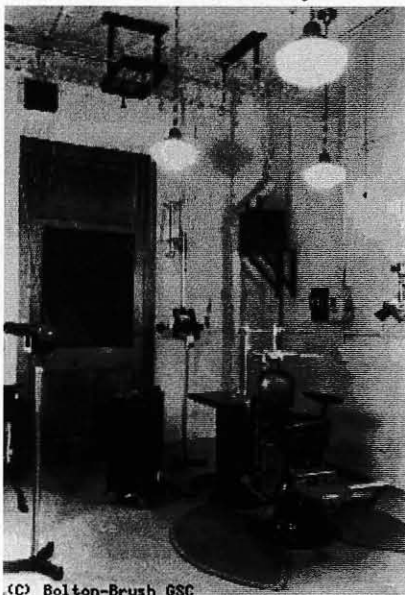
(C) Bolton-Brush GSC

importantly eliminating the uncertainty of measuring changes by comparing the dimensions of different individuals of successive ages.[1]

Broadbent's cephalostat currently resides in the Bolton Room at the Case Western Reserve University Dental School. Although possessing a gothic look and appearing slightly outdated, this cephalostat not only shares but is the origin of standards used by all modern

2

day cephalostats (Figure 3). These standards born in the Bolton Room; consist of patient head position, source-to-object distance, and object-to-detector distance. To be exact, in North America the patient's left side is positioned toward the detector. This detector is fifteen centimeters away from the mid sagittal plane and consists of an extra-oral film, intensifying screen, a cassette, a grid, and a soft tissue shield. [2] With a focus-to-film distance of 152.4 centimeters, a fixed x-ray source, and a patient position this form of

Figure 4: General relationship of film, patients head, and tube for cephalometric radiography
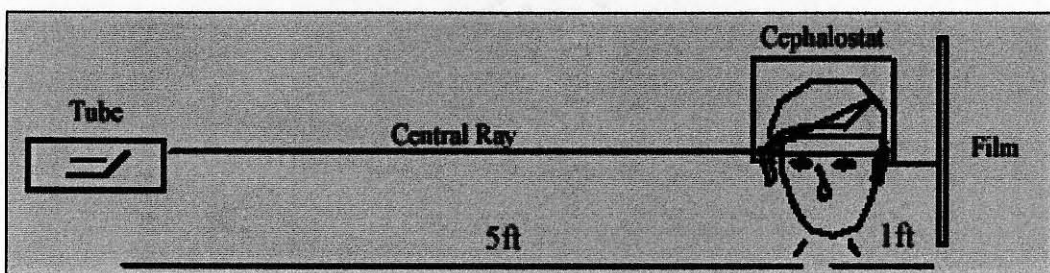
lateral cephalometry is a recipe for repeatable and reproducible images (Figure 4). After x-ray exposure, the conversion of exposed silver halide crystals to metallic silver by chemical processing produces a radiographic image on the x-ray film. [2] Over the years numerous cephalometer imaging system have been developed. However, Orthodontics still largely depends on Broadbent's technique for diagnosis, treatment planning, and patient/parent education ever since.

Computer Radiography

For years conventional radiography was a mainstay since its discovery by Wilhelm Conrad Röntgen, Rector of the Physics Institute, Würzburg, Germany, in 1895.

Not long after Röntgen's discovery there were experiments with storage phosphor technology to create visible area illumination images from invisible ultraviolet aerial images.[45] During World War II, infared-stimuable storage phosphors were used in night-vision cameras, in which an infrared scene image onto a previously energized detector would cause the detector to release its energy as a visible-light replica of the invisible input.[45] In 1981, Fuji (Fuji Photo Film Co. Ltd., Kanagawa, Japan) introduced its digital radiographic system, using photostimuable phosphors as the storage capability for the latent radiographic image.[4, 5] Sonoda et al., began referring to the product as Computed Radiography (CR). Sonoda *et al.*, also predicted that digital radiography would not only compete with but also replace conventional silver-halide film based X-ray technology.[3] This prediction was inspired by the success of computed tomography (CT), new methods of radiographic imaging utilizing recent advances in electronics and computer technology, and the evolution of new diagnostic modalities.[3]

There are two main types of digital systems for dental radiology: direct and indirect. Direct systems place a solid-state detector such as a CCD (charged-couple device) in the patient's mouth. The sensor is connected to the computer via a cable. It responds to x-ray photons and is divided into pixels sized from 20μm-130μm. Most dental systems use this technology. CMOS (complementary metal oxide semiconductor) and amorphous silicon detectors are alternative solid-state technologies that digitize the image at the sensor, not in the computer.

The advantages of direct systems over the phosphor-imaging systems are that a direct image takes just a few seconds to be generated. There is no intervening step

between exposure and reading the image. The sensor can be left in place while waiting for the results.

The charged-coupled device (CCD) requires a scintillator to convert x-rays into light. Once this is achieved, the light passes to the CCD where exposure releases electrons that are then captured in positively charged electron wells. This initiates an electronic circuit to open and in microseconds an electrical signal is produced. Due to a lack of storage capacity, CCD sensors must directly divert its information to a computer to store and view the data. This data is then viewed on a computer monitor as quickly as the signal was produced. CCD sensors were initially quite bulky in comparison to conventional x-ray film which obviously is not a major consideration in extra-oral radiography.[6]

Complimentary metal oxide semiconductor (CMOS) detectors are most commonly used in digital camera and computers.[6] As with CCD chips, CMOS chips lack any storage capacity and both directly relay signals that are stored in a computer to be viewed on a monitor. Early CMOS detectors had increased noise (less sharpness) and reduced space to hold data due to possessing multiple components on the same chip.[6] This is no longer the case. Currently, CMOS chips are not used for panoramic dental radiography because of image transmission timing problems when scanographic systems are applied.

Photostimuable phosphor (PSP) Computed Radiography (CR)

Indirect systems mainly use photostimulating phosphor-imaging plates that are similar in size to conventional film. These are exposed, and then transferred to a solid-

state laser scanner where they are read into the computer. Like any system, photostimuable phosphor (PSP) systems present both a series of disadvantages and advantages. Disadvantages encountered are mostly attributed to the system's automated image acquisition process including an occasional inability to handle collimated images and difficulty for the user to interpret exposure levels recorded on the images.[4] Cowen stressed steps being taken by equipment suppliers and manufacturers to resolve these problems.[4] In contrast to film, photostimuable phosphor (PSP) systems are said to present several advantages supporting their use in digital radiography. These consist of highly reliable image reproduction, ease of data storage and retrieval, lack of need for chemical processing, and possible x-ray exposure reduction to patients.

The make up of a photostimuable phosphor (PSP) system consists of an imaging plate, an image reader, and an image processor (Figure 5). This is a key advantage over its analog competitors because the individual stages can be optimized independently.[45] The imaging plates are made available in every applicable size of conventional intra-oral, panoramic, and cephalometric radiology. Current available photostimuable phosphor systems include the DenOptix system by Gendex (DesPlaines, Illinois), the Orex Paxorama system by Digident (Nesher, Israel), the Digora system by Soredex (Helsinki, Finland), and the Scan X system by Air Techniques Corporation (Hicksville, NY). The flexible imaging plate consists of several layers that as a whole act as the x-ray detector. X-rays first penetrate a protective layer and then enter a phosphor layer consisting of barium fluorohalide (BaFX: Eu^{2+}, where X = Cl,Br, or I) crystals, doped with bivalent europium ions. The remaining two layers of the imaging plate consist of a support layer and a backing layer.
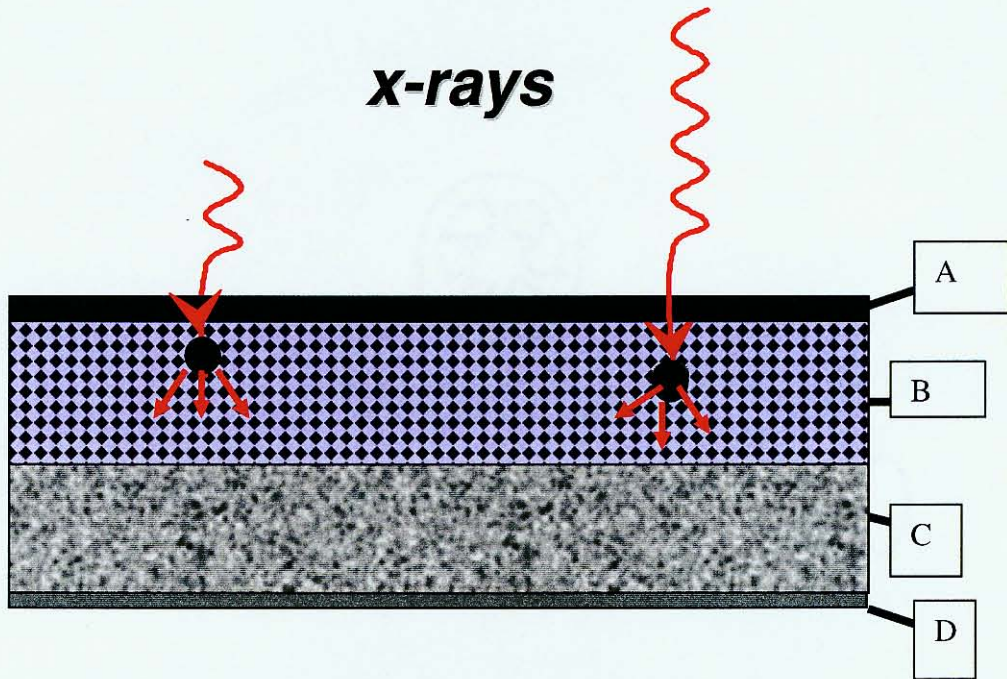
Figure 5: Structure of Photostimuable Phosphor Imaging Plate. (A. Protective layer B. Phosphor layer containing the BaFX crystals C. Support D. Backing)

Two "centers" play a pivotal role in storing the radiographic information. The first center is known as the F center and is formed during X-ray or UV-ray irradiation. Electrons replace specific atoms in the BaFX crystal once trapped in the F center. The second "center" created is a luminescent center formed by the europium ions. These europium ions in the BaFX crystal are ionized, converting from bivalence (Eu^{2+}) to trivalence (Eu^{3+}), during this primary excitation by x-rays. Both the F and luminescent centers play a significant role in storing latent radiographic information[7] (Figure 6). Other materials, such as $RbBr:Tl^{+}$ and $CsBr:Eu^{2+}$, have been or are being used as storage phosphor

materials in CR systems. There is still much active research into finding new and optimizing current materials.[45]

Figure 6: Crystal Structure of BaFX (X = Cl, Br, I)
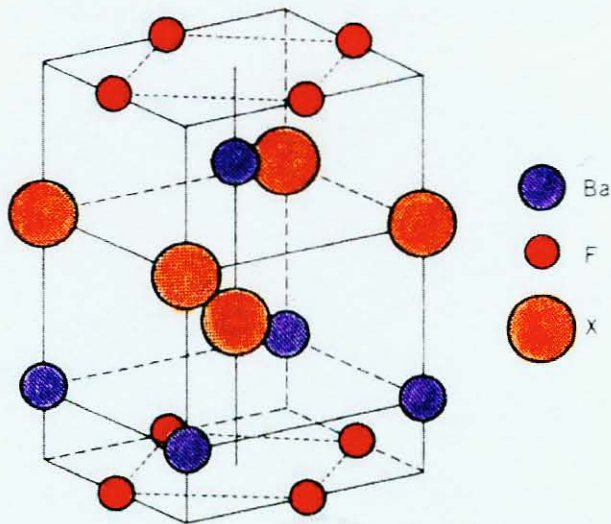
Secondary excitation occurs when a laser is used to scan the latent radiographic image stored in the imaging plate (Figure 7). [8] Initially He-Ne lasers (633nm) were applies but now solid-state lasers are used. There are also storage phosphor scanners in development (Agfa, Fuji) that abandon the point-by-point method of reading and instead read an entire line of data points at once, enabling considerably faster CR systems than those commercially available today.[45] The previously captured electrons are temporarily released from the F centers and then captured again, this time by the trivalent europium ions (Eu^{3+}). Energy is then released as a fluorescent blue light luminescence. This light

is focused on the input plane of a photomultiplier tube, resulting in a photoelectric current that is then amplified. This current passes through an analog to digital (A/D) converter producing a digital signal that could be stored in computer memory for monitor display or enhancement.[9]
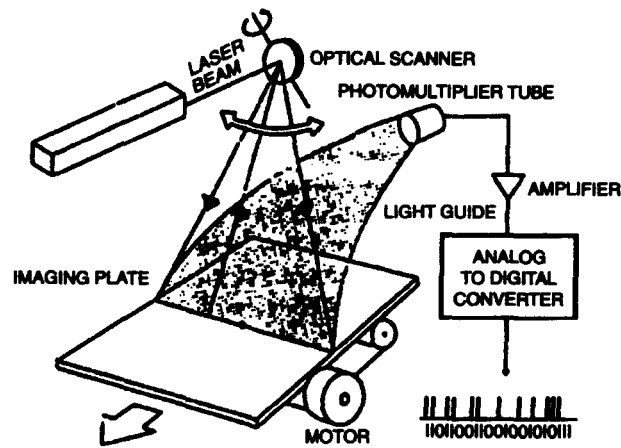
Figure 7: Construction of the Image Reading System

Computed and conventional radiographic images are quite similar in regards to the ultimate product, a radiographic image of any specific object. However, the paths taken acquiring an image and how the image is displayed are quite different. In Fact, trying to equate the two techniques may often prove to be like comparing apples and oranges.

Conventional radiography takes an exposed film and chemically processes it. This processing converts the exposed silver halide crystals within the film's emulsion layer into grains of metallic silver. This processing technique is responsible for the film's gray scale appearance. With gray scale meaning the overall degree of blackened or

darkened appearance, this is the density of the film radiograph. The density of the film is defined as:

$$\text{Density} = \log_{10} I_o/I_t$$

With a density of 0, 100% of the incident light is transmitted through the developed film. With a density of 1, 10% of the incident light is transmitted through the developed film. With a density of 2, 1% of the incident light is transmitted through the developed film. The useful range of densities for conventional film radiographs was controversial, but generally accepted to be within the 0.3 (light) and 2 (dark) range. Anything outside this range could be too dark or too light to be diagnostically useful.[6]

A curve exists used to show the exposure properties of a film or a film screen system. The characteristic curve, which was described in 1890 by Hurter and Driffield, is a representation of how the exposure of the film is related to the measurable signal, i.e. the blackening of the film, or film density. The characteristic curve is different for different film types but has a general shape as shown in Figure 8.
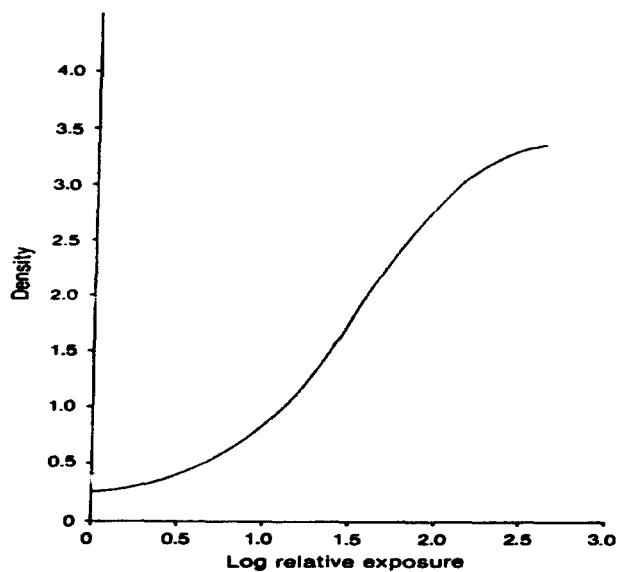
Figure 8: The Characteristic Curve of Conventional Film

The base and fog density is measured on an unexposed film. The shape of the characteristic curve tells the user the contrast properties (slope of the linear part) and the useful exposure range (length of the linear part). It also will indicate the speed of the film (or film-screen system), which can be judged from the curve's position along the horizontal axis. The speed class can also be found from the characteristic curve.[10] If the slope of the curve that is in the useful range, called the film gamma, is greater than 1, the film exhibits exaggerated contrast. This is a desirable feature found in most direct exposure film to allow visualization of structures that may have similar densities. Films using intensifying screens (e.g. panoramic and cephalometric films) have film gammas in the range of 2 to 3.[6]

When comparing conventional radiography with computed radiography a major problem is encountered. The problem being that the characteristic curve is not applicable to computed radiography. The reason for this is that computed radiography uses a computer monitor or a hard copy 2-dimensional printed image to display an image while conventional radiography uses the transmittance of light through film. Instead measurements of signal dependence on sensor or imaging plate exposure are used to assess the total system response using computed radiography. This is done by using the luminance (L) value of a computer monitor dependent on the voltage (V) level supplies to the system (Figure 9).
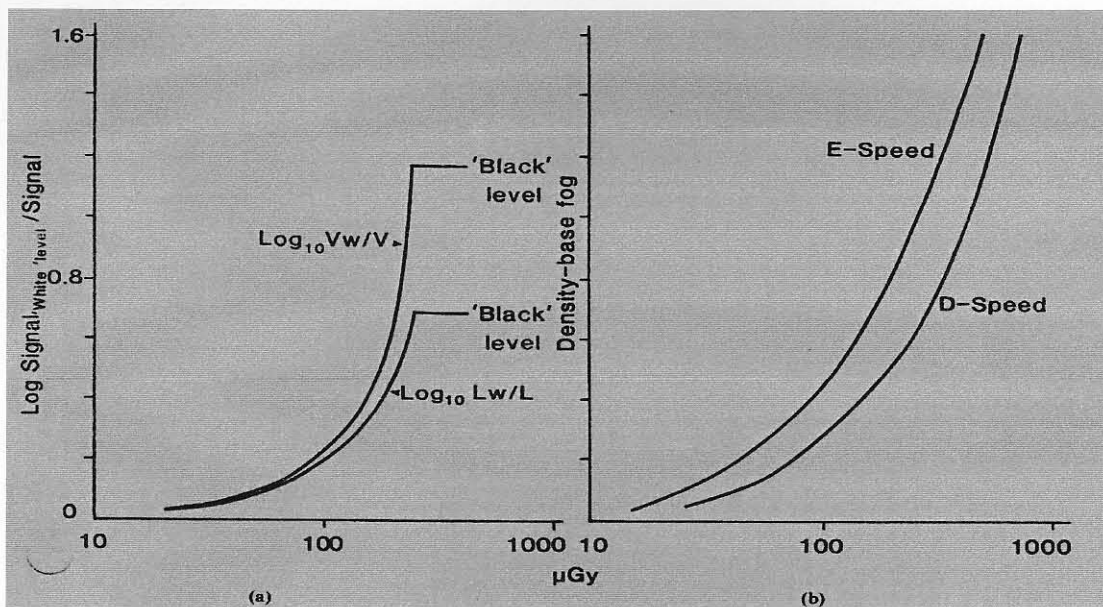
Figure 9: Characteristic Curve for Conventional X-ray Images and an Analog For Digital Images

Log V_w/V provides information about the contrast and latitude available at the image signal level and Log L_w/L showed how this information is reproduced on the screen of the monitor:

Log V_w/V and log L_w/L

Pixel value can act as the density-equivalent and be plotted against the log of the exposure as another method of comparison to the characteristic curve. Unfortunately there is no direct relationship between the measured pixel value and phosphor exposure of the storage phosphor plates as there is with exposure and density of direct exposure film (characteristic curve). Methods to compare the two types of media in relation to contrast, latitude and speed still need to be standardized. The relationship between pixel value and exposure (Figure 10) is sometimes used with digital imaging systems, transforming measured signal intensities into pixel values.

12
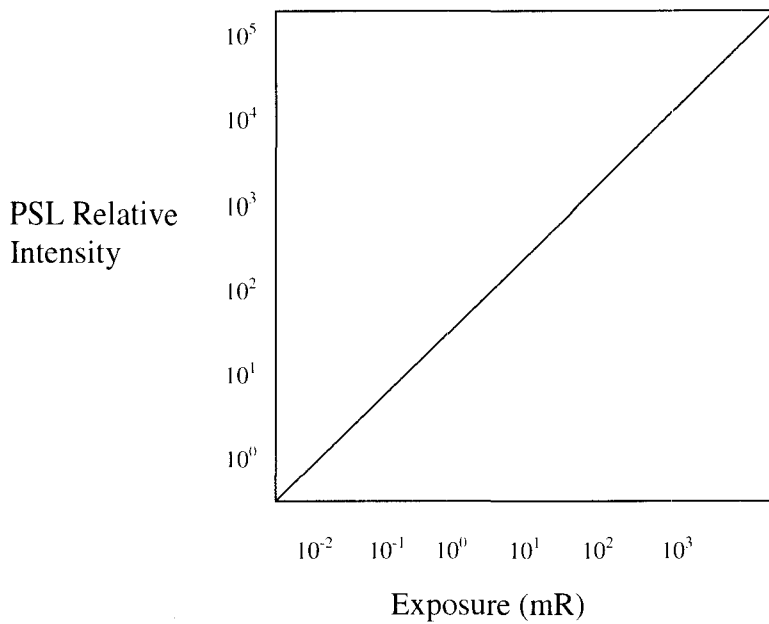
Figure 10: The Relationship Between Pixel Value and X-ray Exposure

Storage phosphor systems do exhibit an improved low contrast detectability

performance as a result of higher x-ray detection efficiency. The exposure level for the

image can be quite low, however, the signal-to-noise ratio is a limiting factor for image

quality at very low exposures. Conversely, in theory, the radiation exposure used with

storage phosphors can be increased to a greater degree without having to worry about

overexposing the image.[11]

Computed Radiography has come a long way in about 20 years, from laboratory

curiosity to mainstream imaging uses. The reliable current systems are approaching their

physical limits with regard to factors such as image quality and scan speed. New

approaches to computed radiography must be considered and some do currently exist.

The main new developments include dual-sided reading, structured storage phosphors

(needle image plates), and line scanning. Dual-sided reading refers to detecting emitted light from both sides of the imaging plate to extract more signal and improve the signal-to-noise-ratio. Structured storage phosphors are grown under carefully controlled temperature, pressure, and mechanical conditions to form long crystalline rods or needles. In summary these needles allow for improved image sharpness, x-ray absorption, and decrease screen structure noise. Line scanning uses a row of solid-state laser instead of a single laser. The stimulation sources, beam-shaping optics, light collection optics, filters, and photodetectors are all contained in a scanning head that is as wide as the screen. The entire screen surface is scanned through a relatively linear movement of the head and the screen. This improvement allows for a much smaller CR system. Furthermore, luminescence decay is no longer an issue along with an overall improvement in the photodetectors collection efficiency. Photostimuable phosphor systems may be considered familiar and old technology by some, however it is actually still dynamic and has the potential for considerable improvement and optimization in the future.[45]

Radiographic Contrast

Photostimuable phosphor images have been shown to have an improved low contrast detection performance in comparison to traditional film radiographs.[12] This low contrast detection performance is a result of higher x-ray detection efficiency. Contrast refers to the difference between light and dark regions of a radiograph. A high contrast radiograph possesses fewer shades of gray only displaying very light and very dark areas

14

(Figure 11). The fewer shades of gray involved, the shorter the image's gray scale. Conversely, a long gray scale is associated with a low contrast image. Low contrast is attributed to a higher efficiency in x-ray detection than the lower detection efficiency of a high contrast radiograph (Figure 12). Many factors influence the degree of contrast achieved by an image. These factors include the object being radiographed, the recording medium, and fog created by several other inadequacies.

Figure 11: Extremely High Contrast.

Figure 12: Extremely Low Contrast

Contrast affected by the particular object being radiographed is referred to as subject contrast. Subject contrast is dependent on 1) the composition and physical properties of the subject and 2) the energy of the x-ray beam *(kV)*. Most orthodontists preferred to use *kV* values in the 60-90 ranges. [10]

The characteristics of the recording medium will also play a role in the contrast of a radiograph. The contrast will depend on a film emulsion's response to the x-ray beam. This response is based on 1) the characteristic curve of the film 2) the film density 3) the intensifying screens used (for traditional film radiography) and 4) film processing (for traditional radiography). In computed radiography these film characteristics are

substituted by the type of phosphor plate used along with the specific algorithms employed in producing the "for processing" and "for presentation" images.

As previously mentioned fog also referred to as noise may also affect contrast in either conventional radiographs or computed radiographs. This noise may be caused by scattered radiation, processing conditions, and film/plate handling. Scatter radiation results in a darkening of both conventional film and phosphor plates causing a decrease in contrast. Exposure to visible light prior to processing will result in darkening conventional film while lightening phosphor images. This being the reason light is used to erase phosphor plates so that they may be reused. [11]

A recording medium can have a wide dynamic range if the range of x-ray energies and quantities passing through an object can be usefully recorded while representing all density variations of an image proportionately and in detail. The dynamic range for x-ray film is 10^3:1.[13] This means that a black image is produced by a given radiation dose 1000 times greater than the radiation dose that it took to produce a white image. The dynamic range for the storage phosphor system is reported to be much wider. Its dynamic range is reported to be 10^4:1[9] The ability to record a series of distinguishable densities on a film is known as film latitude. Film with wide latitude is able to record an object with a high or wide contrast. An H&D curve that exhibited a long straight-line portion and a shallow slope is characteristic of film with wide latitude. The wider the recording latitude, the greater the range of densities that can be visualized. Films with wide recording latitudes also show low contrast and long gray scales. This is useful when trying to distinguish between dense osseous structures and soft tissues of the facial region as used in orthodontic cephalometric radiographs. With conventional film radiography, altering the

beam energy will alter the film latitude. Using high beam energy would produce a film with a wide latitude and low contrast. Using reduced exposure time will result in an image that is lighter and possesses wider latitude.[15]

Unlike conventional film, the photostimulated light emission of the imaging plate is converted to electric signals with the photomultiplier tube. This allows for computed radiography to produce a wider dynamic range. As long as the information on a phosphor plate is completely transferred digitally to computer memory, a substantial increase of information can be used for diagnostic purposes. Tissues of varying densities and attenuating properties (i.e. soft tissue, bone) theoretically can be accurately recorded with this technique. Having a wide dynamic range allows digital radiographs to be obtained under a wide array of operating conditions and beam energies. With these varying conditions, small differences in x-ray absorption of tissue types can still be detected. Exposure latitude is probably the biggest difference between and the most important advantage of digital radiographs over conventional film radiographs.[9]

Signal to Noise Ratio

Noise in computed radiography can negatively affect the ability of an imaging system to accurately reproduce details and the observer's ability to detect details. A Conventional x-ray film uses chemical processing to obtain a final image while a photostimuable phosphor system uses a laser scanner to obtain its final image. This laser scanner converts the information stored on an imaging plate into electrical signals. This conversion of an x-ray analog signal into a digital signal creates what is referred to as a

signal-to-noise (SN) ratio. This ratio refers to the ability of the useful signal to be exhibited in spite of background interference. The signal-to-noise ratio can be used in computed radiography to calculate the ratio between image forming signal (average pixel value) and the noise (standard deviation) using plain exposure fields.

Noise may arise either during the image acquisition or image display processes. Sources of quantum noise include x-ray source, the stimulated light emission quantum noise of the imaging plate when it is laser scanned, the structural noise of the imaging plate, optical noise, electric noise and the inherent noise of the computed radiography system itself including effects of scanning pitch selection. Cowen collected that due to its wide dynamic range, the storage phosphor system's noise source depends on the signal level within a specific range[4]. At low exposure quantum noise may be the main source, while at high exposure structure mottle and reader noise are of main concern.[4] Displaying images on monitors creates electronic noise and raster jitter while other electronic sources create noise through circuit transmission and heat.[4]

Dose Reduction

Past research strongly supports a reduction in radiation dose to the patient when applying photostimuable phosphor system to cephalometry. In 1988 Kogutt published a study considering image quality and radiation reduction using photostimuable phosphors plates for pediatric chest images. This study showed an 85% reduction in radiation dose compared to conventional images, with 94% of digital images rated satisfactory.[15] In 1993, Seki and Okano further supported an extreme reduction in radiation dose of

photostimuable phosphors in comparison to conventional radiographs. As the case for

Kogutt, this exposure reduction did not compensate clinical application.[16]

Huda et al. directly compared the photostimuable phosphor system with E-speed direct

exposure x-ray film for intra-oral radiography. By measuring the direct response of each

system as a function of radiation exposure, Huda concluded photostimuable phosphor

detectors low contrast object detection superior to x-ray film.[87] In 1997, Lim compared

phosphor-stimulated computed cephalometry to conventional lateral cephalometry in a

randomized, controlled, prospective study and found that computed lateral cephalograms

had made a 30% radiation reduction without clinically significant differences in landmark

identification.[17] Almost one year later, Näslund found that a reduction in x-ray dose with

computed radiography of 75% compared with normal exposures did not affect the

localization of anatomical landmarks in lateral cephalograms.[18]

Landmark Detection

Stressed by the importance of Broadbent's cephalostat, orthodontics depends on

the lateral cephalogram for diagnosis, treatment planning, and review purposes.

Unfortunately the identification of hard and soft tissue landmarks is not flawless. Error

may occur due to superimposition of structures, blurring of images due to patient

movement, lack of film contrast, and human perception erros.[22] In 1984 Cohen publish

the appropriately named article "Uncertainty in cephalometrics." This article highlighted

two major errors with cephalometric radiography. This first error being systematic and

implying a bias in the recording and measuring system to produce apparent measurements predictably different from the true ones. Cohen explained the second error as random and arising through uncertainty in the observers' identification of radiographic landmarks.[19] In 1994 Tng found a statistical difference between cephalometric landmarks estimated on cephalograms from the true landmarks on dry skulls. Hagg also compared cephalometric landmarks on dry skulls and regular cephalograms to find less digitizing errors with the dry skull cephalograms. This finding was attributed to soft tissue influences on landmark clarity.[21] Research obviously supports that orthodontics has been plagued by the uncertainty of information in the lateral cephalogram.

With image quality being a major concern, understanding the parameters of digital images is important. Image quality can be affected by matrix size, unsharpness in the underlying image, bit depth, and noise in the underlying image. As do the display mediums between analog and digital images, differences between the actual expressions of the images also exist. An analog image is a continuous distribution of densities that may be compared to the continuous light intensity ranges found in an art painting such as da Vinci's Mona Lisa.

Figure 13: da Vinci's "Mona Lisa"

Figure 14: Magnified Mona Lisa displaying continuous densities

In contrast to analog images, a digital image is made up of discrete points or pixels of varying density. This was analogous to the point of color art painting style used by the pointillists, such as Seurat.[24]

Figure 15: Seurat's method of Pointillism in "Sunday Afternoon on the Island of La Grande Jatte"
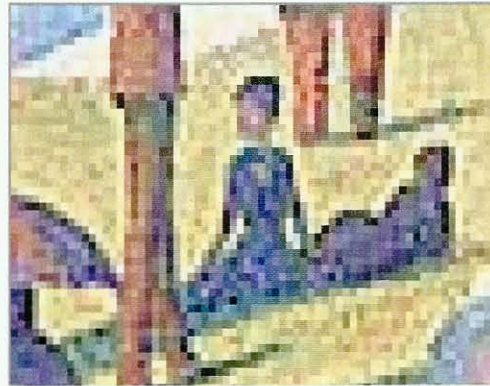
Figure 16: Magnified digital image of Seurat painting displaying individual pixels. Pointillist paintings use dots of paint that are comparable to such pixels

A photostimuable phosphor system creates a latent analog image that must be converted to digital for computer storage and processing. This latent image must first go through a process called spatial sampling. Spatial sampling divides the image into many individual boxes referred to as pixels. The array of all the pixels of the image is organized into an image matrix. An example of a simple matrix is a 2 x 2 (2^2). The image could be divided into four separate pixels representing the average density of the corresponding region of the original image. The average density of the structures within each pixel determined its gray value. Such an image would not have been very representative of the original image due to the very small matrix. As each individual pixel is made smaller, more of the original details of the image become visible. Actual digital images are typically divided into 1024 rows and 1024 columns of pixels, corresponding to a 1024 x 1024 matrix. A 512 x 512 matrix is common as well but is not

recommended for digital cephalometric images due to the inferior spatial resolution for a given image dimension.[11]

As the pixel size decreases the number of pixels that form the image increases. Mathematically, for the square image matrix the total number of pixels quadruples every time the width of a pixel is divided in half. If the number of pixels is too small the resolution of the image suffers. However, the use of too many pixels may be impractical when considering storage space in the computer. The digital image that is composed of many pixels will slow the passage of a complete image through an image processor of a computer.[11]

The number of pixels that are required to display an image are determined by the size of the pixel and the size of the image. The larger the image to be displayed, the more pixels required to represent the image at a desired resolution. The size of the individual pixel determines the resolution of the image. The total number of pixels multiplied by the pixel size determines what is called the field of view. In a fixed matrix as the size of the pixel increases the field of view increased causing a decrease in the resolution. The size of the pixel also affects the spatial resolution of the image.[11]

Image Sharpness refers to an images ability to disclose small or fine details. Spatial resolution is characterized by its modulation transfer function (MTF) that described its response over a range of spatial frequencies. Noise in radiographic images is quantified by the measurement of the noise power spectrum of the images. This power spectrum is a measure of the noise power as a function of spatial frequency.[6]

For digital imaging including storage phosphor images spatial resolution is determined by the modulation transfer function (MTF) that describes its response over a

range of spatial frequencies at various contrast levels.[18, 24,28,29] The unsharpness of the

storage phosphor image is determined by: the diameter of the laser scanning pitch,

scattering of the laser onto adjacent areas of the imaging plate, x radiation scatter and

reabsorption within the imaging plate, analog electronic signal processing and the digital

sampling interval. Scattering of light of the laser onto the imaging plate and the diameter

of the laser (pitch) are the primary factors in determining spatial resolution of the digital

images.[30] Low dose radiology produces images with an increased amount of noise due to

quantum mottle (a fluctuation in x-rays). [31]

Each pixel has a digital value that represents the intensity (radiodensities) of the

information recorded. Each digital value is represented as a binary number. This

information is stored as a series of 1's or 0's. Each one or zero is called a bit. In an 8-bit

image a pixel could have 256 possible values (2^8), from zero that represents black to 255

that represents white on the image. A 16-bit (2^{16}) image could have 65,536 possible

values with a similar representation of values.[25, 26]

Previous work carried out by various researchers within the Radiology laboratory

of Dr. Allan G. Farman at the University of Louisville has demonstrated that DenOptix

(Gendex, Des Plaines, IL) images have one of two basic image histogram distributions,

namely, single peak and double peak.[32] The histogram is a tool that allows a display of

the gray levels for a given image. Each peak corresponds to either soft tissue or hard

tissue depending where in the spectrum the peak is located. In a 16-bit image the soft

tissues peak is to the left in the histogram in the 25,000-30,000 gray level range and the

hard tissue peak is to the far right of the histogram in the 58,000-65,500 gray level range

(a twin peak image). The absence of the soft tissue peak (a single peak image) is

indicative of the absence of soft tissues display for the given image. In other words the image is overexposed and there are not any detectable pixel values for the soft tissue gray level scale.[27] This information is particularly relevant for these two forms of DenOptix images have been utilized in this study.

Storage of Digital Images

There are many different formats available for storing image files. Some of the most common include: Tagged Image File format (TIFF), Joint Photographers Expert Group (JPEG), Standard Windows Bitmap (BMP), CompuServe Graphics Interface Format (GIF) and Digital Image Communication in Medicine (DICOM). [11]

The TIFF image is a very good format to acquire image data because no information need be lost. TIFF images can be transported from one application to another or from one computer to another as they were designed to be independent of any particular software or hardware. Another advantage to these types of images is that, if enough space exists on a computer's hard drive they are useful to keep as an archive permitting modification to another file format in the future. One disadvantage of the TIFF format is that the file size is large and, therefore, takes up much space when stored and sometimes requires a long time to open with the application software that was utilized. Cheaper, faster storage and processors has made these problems less important than before. Compression became most important with respect to reducing transmission times in teleradiology and in reducing the needed bandwidth of the transmission channel.[11]

Post-processing of Images

Post-processing capabilities of photostimuable phosphor systems are another added advantage against conventional radiography. With conventional radiography the x-ray film acts not only as the sensor but also the display medium. In Layman's terms, what you see is what you get. The only form of enhancement possible must involve secondary digitization. With storage phosphor systems the sensor and display medium are separate entities. The imaging plate acts as the sensor while a computer and monitor act as the storage and display medium. Once stored the image can be viewed and altered like most computer files. Manipulation of the displayed image can involve several enhancement techniques by use of various algorithms. These enhancements techniques include window and level selection, gamma correction, contrast manipulation, edge-enhancement, subtraction, colorization and 3-D reconstruction.[15]

Studies have indicated the quality of the radiographic image is the most important factor in affecting the reproducibility of accurate detection of cephalometric landmarks. Digital imaging quality can be influenced by contrast enhancement and sharpening if images are obtained through digital processing.[33, 32, 34]

Researchers at the Veterans Administration and the University of Maryland, Baltimore have demonstrated potential use for photostimuable phosphor post-processing enhancement in the detection to lung tumors. By adding a specific contrast enhancement, an increase in lung cancer detection accuracy was achieved.[35]

Enhanced color images from electronic videoendoscopic evaluation of laryngeal lesions with digital image processing have shown to be superior in both quality and resolution to those obtained by electronic videoendoscopy without digital processing and enhancement (Kawaida, 2002).[36] Oral implantologist usually use panoramic radiographs for the evaluation of bone tissue around implants. The development of computed tomography combined with computer software has allowed for the bone-to-implant interface to be illustrated in greater detail with cross-sectional and pseudo-color images (Bocklage, 2001).[37]

Researchers within the Radiology laboratory of Dr. Allan Farman at the University of Louisville used post processing software VixWin2.3 (Gendex®, DenOptix™, Des Plaines, Illinois) to enhance lateral cephalograms. These enhancements consisted of emboss (a 3-D presentation), inverse and inverse emboss techniques. Postprocesssing enhancements made it possible to more readily and clearly detect landmarks and detect them more efficiently than in conventional methods.[6]

This VixWin 2.3 software (Gendex®, DenOptix™, Des Plaines, Illinois), is the software used in the present study for post-processing. Obviously from West's thesis, emboss and inverse are two enhancement techniques which may be utilized with this software. Another contrast enhancement capability includes colorization of the black and white image. This colorization along with emboss and a combination of the two will be the focus of the present study.

Overview

The previously mentioned reports obviously support several potential advantages for photostimuable phosphor systems, including potential decrease in the overall dosage of radiation to expose the patient, improvement in image quality, post-processing and management of the image after the radiograph is taken, elimination of chemical processing required by conventional radiographs, and decrease of the complexity and space needed for records.[38, 39, 40]

The purpose of this study is to further explore the value of photostimuable phosphors in digital lateral cephalometry focusing in the areas of landmark identification for diagnosis and treatment of orthodontic malocclusions. The study aims to determine what other new and radiographic technique is superior to traditional radiography given its enhancement capabilities.

Chapter II

Purpose

The purpose of this study is to establish whether a difference in quality of

depicting cephalometric landmarks and their detection by observers exists by using image

enhancements in photostimulable phosphor cephalograms having three different

histogram distribution/bit depth configurations.

Research Question and Hypothesis

Research Question: To determine whether specific image enhancements improve

detection and quality of specific anatomic landmarks used in cephalometry.

Specific Objectives: To evaluate 8-bit and 16-bit photostimulable phosphor

cephalograms for orthodontists' perceptions of quality of twelve specific cephalometric

landmarks clarity and overall image quality under the following enhancement conditions:

(1) No enhancement; (2) Embossing the image; (3) Colorizing the image; and (4)

Embossing and colorizing the image.

Specific Aims: SA1: To determine if a difference exists among non-enhanced images

and images presented in emboss, colorized, and a combination of emboss colorized

format for cephalometric landmark detection and quality among histogram distributions.

SA1 Null Hypothesis: No difference exists among non-enhanced cephalometric

images and images presented in emboss, colorized, and a combination of emboss

colorized for anatomic landmark detection among pixel histogram distribution.

SA1 Alternative Hypothesis: A difference exists among non-enhanced

cephalometric images and images presented in emboss, colorized, and a combination of

emboss colorized format for anatomic landmark detection among pixel histogram distribution.

Specific Aim: SA2: To determine if a difference exists among non-enhanced images and images presented in emboss, colorized, and a combination of emboss colorized format for overall quality of the cephalograms among histogram distributions.

SA2 Null Hypothesis: No difference exists among presentation of non-enhanced cephalogram images and images presented in emboss, colorized, and a combination of emboss colorized format for overall quality of the cephalograms among histogram distribution.

SA2 Alternative Hypothesis: A difference exists among presentation of non-enhanced cephalogram images and images presented in emboss, colorized, and a combination of emboss colorized format for overall quality of the cephalograms among histogram distribution.

CHAPTER III

STUDY DESIGN

Sample

The patient sample consisted of Orthodontic patients presenting for cephalometric imaging in the Radiology Clinic, The University of Louisville between June and October 2000. Informed consent was obtained under IRB approval # 330-00.[27]   Twelve cephalograms were selected from this sample according to the histogram distributions of the pixels and bit depth.

Radiographic Technique

All digital images were created with the Quint Sectagraph (Denar Corporation, California), (Figure 17) operating at 70 kV and 200 mA at the large focal spot setting with 2 mm aluminum equivalent filtration.

Figure 17. **Quint Sectagraph QS-325**

The imaging plates used in this study were photostimulable phosphors

manufactured by Fuji Medical Corporation, Tokyo, Japan for Gendex (Des Plaines,

Illinois). The size of the imaging plates was 8"x 10". Immediately prior to x-ray

exposure the imaging plates were saturated with > 4000 lumens fluorescent light. After

the imaging plate was exposed to x-radiation the imaging plate was removed from the

cassette under subdued ambient light of < 18 lumens and placed into the DenOptix laser

scanner, (Gendex, Des Plaines, Illinois), (Figure 18), for scanning of the latent image to

produce photoluminescence. The photomultiplied analog image was digitized and

imported into a Gateway 2000 GP5-166 (San Diego, CA) computer using a Microsoft

WINDOWS (Redmond, WA) platform for digital processing.
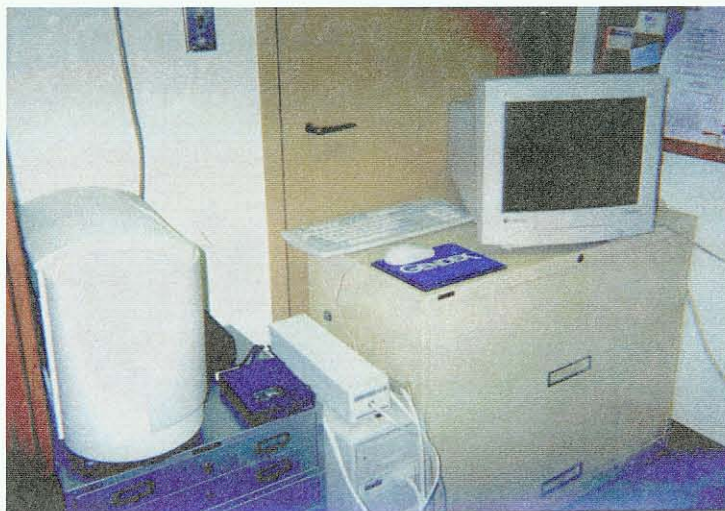
Figure 18. DentOptix Imaging Instrument including DenOptix Scanner/
Gendex/VixWin 2.3

The patient images were acquired at either 0.2 s or 0.15s depending upon patient

size using the same photostimulable phosphor imaging plate and stored both in an 8-bit

and 16-bit Tagged Image File format (TIFF) following laser scanning at 150 dpi utilizing

the DentOptix Imaging Instrument (Dentsply/Gendex, Des Plaines, Illinois), (Figure 18).

Images were exported to a Dell Inspiron 5000 (Dell Computer Corporation, Austin, Texas) for contrast enhancement using VixWin 2.3 software (Gendex® DenOptix™, Des Plaines, Illinois), for the following enhancements (1) No enhancement; (2) Emboss; (3) Colorized; and (4) Emboss and Colorized. The Research Randomizer was used to randomize the 60 total images, which included 12 images for each of the four image states (48) and 12 randomly selected repeat images for purposes of intra-rater reliability determination. [41]

The present study used histogram analysis to evaluate the spectrum of gray levels within an image. The histogram was set for both 8-bit and 16-bit images including single and double peaks and was located within the "Tools" menu of the software used to obtain the image (VixWin 2.3 from Gendex® DenOptix™, Des Plaines, Illinois). [42]

Observation

Images compared included 8-bit single peak, 16-bit single peak, and 16-bit double peak using the previously mentioned enhancement algorithms in each case. The observers comprised a group of 10 raters from the University of Louisville School of Dentistry Orthodontic Department, including nine orthodontic residents and one faculty member excluding all investigators. The landmarks to be identified were chosen to represent a common variety of hard and soft tissue anatomical landmarks (Table 1). The landmarks observed were clearly defined before each session as well as in a handout provided to the raters (Figure 19). Each rater received a handout of instructions and definitions, a descriptive figure (Figure 20) of the landmarks and a chart to record the perceived quality of each landmark together with perception of the overall image quality

(Table 2). The University of Louisville School of Dentistry Simulation Lab was utilized

to permit simultaneous individualized ratings (Figure 21). Formal rater calibration was

preformed prior to collection of the data. Care was taken to include patient cephalograms

initially having both double and single peak histograms.

Table 1. Table of Hard and Soft Tissue Landmarks Observed

Soft Tissue Landmarks	Hard Tissue Landmarks
Labrale Superius	Sella
Labrale Inferius	Nasion
Soft Tissue Pogonion	Porion
Pronasale	Orbitale
	A Point
	B Point
	Pogonion

Figure 19. Landmark definitions provided to all raters

Definitions of the Cephalometric Landmarks Observed

Sella (S) - The midpoint of the pituitary fossa.

Nasion (Na) - The most anterior point of the frontonasal suture in the median plane.

Porion (Po) - Anatomic porion-superior rim of external auditory meatus.

Orbitale (O) - Lowest point on the averaged inferior borders of the bony orbits.

Point A (A) - The point at the deepest midline concavity on the maxilla between the anterior nasal spine and prosthion.

Point B (B) - The point at the deepest midline concavity on the Mandibular symphysis between infradentale and Pogonion.

Pogonion (Pog) - The most anterior point of the bony chin in the median plane.

Pronasale (P) - Tip of the nose.

Labrale Superius (Ls) - The most outward projection of the upper lip.

Labrale Inferius (Li) - The most outward projection of the lower lip.

Soft Tissue Pogonion (Pog') - The most prominent point on the soft tissue contour of the chin.
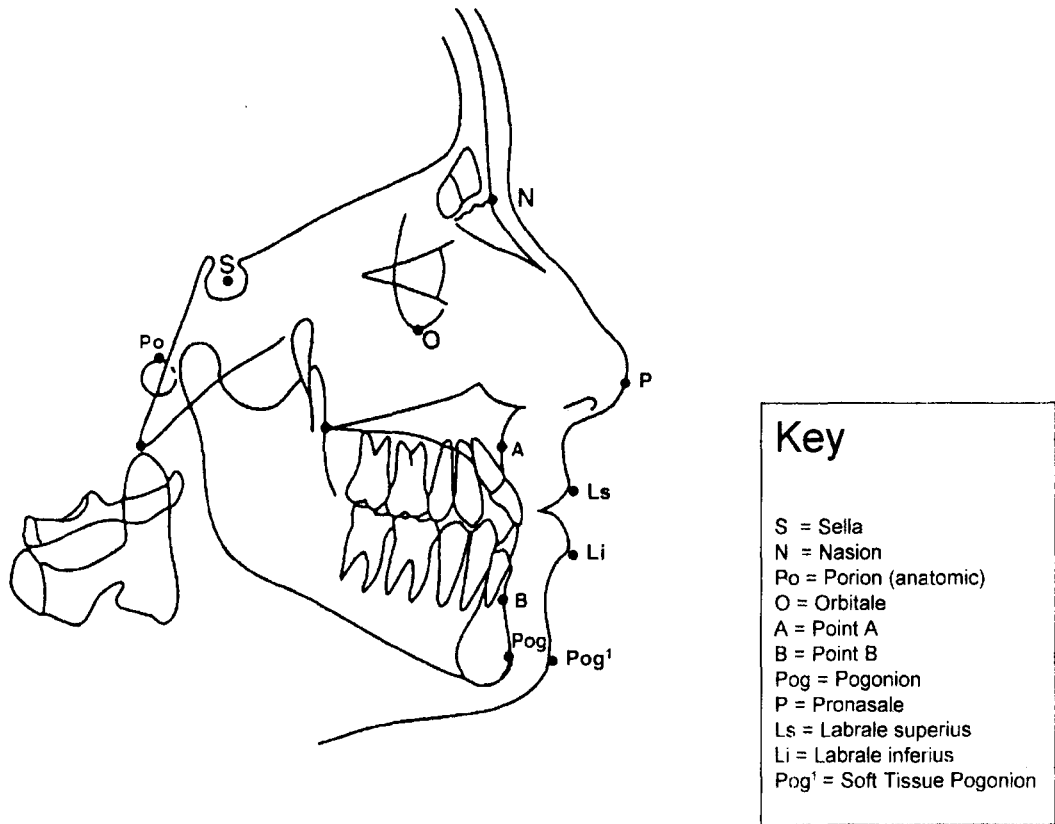
Figure 20. Diagram for Landmark Identification

Key

S = Sella
N = Nasion
Po = Porion (anatomic)
O = Orbitale
A = Point A
B = Point B
Pog = Pogonion
P = Pronasale
Ls = Labrale superius
Li = Labrale inferius
Pog¹ = Soft Tissue Pogonion

Table 2: Perceived quality of each landmark/Perception of the overall image quality

Raters: For the following images please rate the cephalometric points below using a scale of 1-3.

Images 1-11   **12: Overall Image**
1 = cannot see landmark   1=poor
2 = can see landmark but of poor to fair diagnostic quality   2=satisfactory
3 = can see landmark and of fair to excellent diagnostic quality 3=excellent

	1	**2**	**3**
Sella	_____	_____	_____
Nasion	_____	_____	_____
Pt B	_____	_____	_____
Pt A	_____	_____	_____
Labrale Superius	_____	_____	_____
Labrale Inferius	_____	_____	_____
Pronasale	_____	_____	_____
Soft Tissue Pogonion	_____	_____	_____
Pogonion	_____	_____	_____
Porion	_____	_____	_____
Orbitale	_____	_____	_____
Overall Image	_____	_____	_____
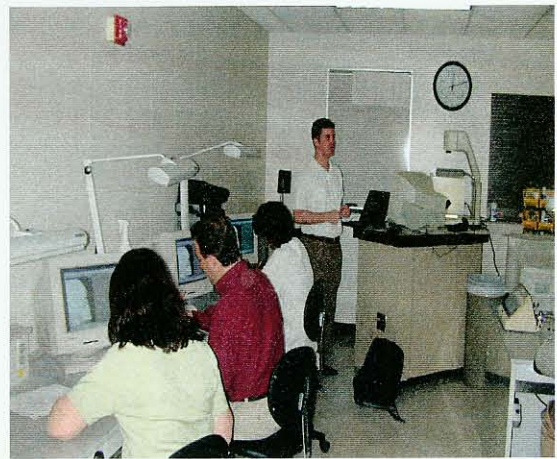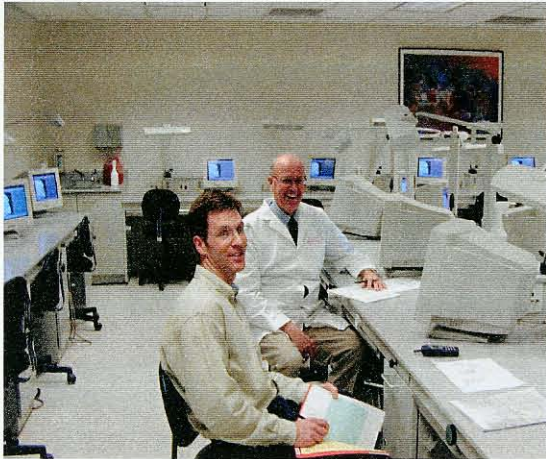
Figure 21. University of Louisville School of Dentistry Simulation Lab

The computer (Pentium III, IBM, Armonk, NY) into which the images were loaded ran on a WINDOWS 2000 platform (Microsoft™, Redmond, Washington). In a darkened room, each rater had their own 17" super VGA monitor (Optiquest Q51, Walnut, CA) with bandwidths between 70 to 80 MHz and a dot pitch of 0.28 mm. This monitor was chosen because it is a common monitor type found in many orthodontic clinical settings and is the type available in the simulation clinic. The computer monitors utilized the 800 x 600 matrix setting. The standardized setting for each computer monitor can be found in Table 3. The super VGA monitors that are commonly utilized for image display in dentistry were capable of displaying an 8-bit image (256 gray levels).

Table 3. Simulation Lab Computer Monitor Settings

CPU	Pentium III, 600 MHz
Operating System	Windows 2000
Contrast	75 %
Brightness	75 %
Monitor	Optiquest Q51

Each rater evaluated the quality of each landmark and whether or not the entire image was of acceptable diagnostic quality. Each rater had approximately one minute to grade all of the points for quality and the overall image quality for each image.

Images presented to raters were of one of three histogram formats: 8-bit, 16-bit single peak, and 16-bit double peak. Along with the three histograms, images were post-processed enhanced and presented as no-enhancements, emboss, colorized, and emboss/colorized. Examples of the 8-bit, 16-bit single peak histogram, and 16-bit double peak histogram along with enhancements are displayed in figure 22- figure 36.

Cephalometric Images

Figure 22: 8-bit not enhanced
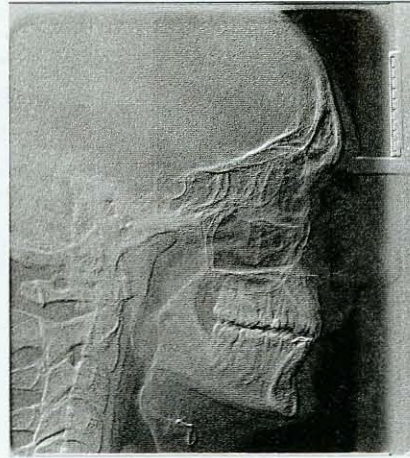
Figure 23: 8-bit emboss
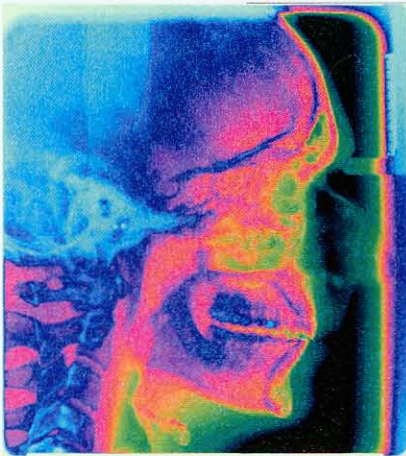
Figure 24: 8-bit colorized
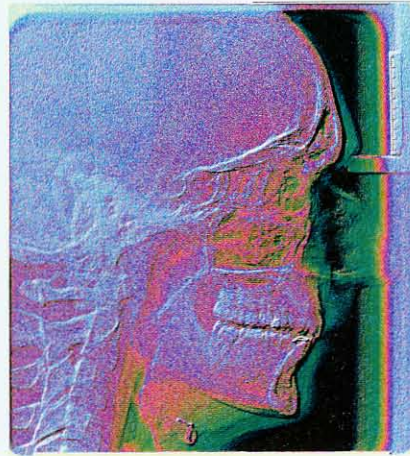
Figure 25: 8-bit emboss/colorized
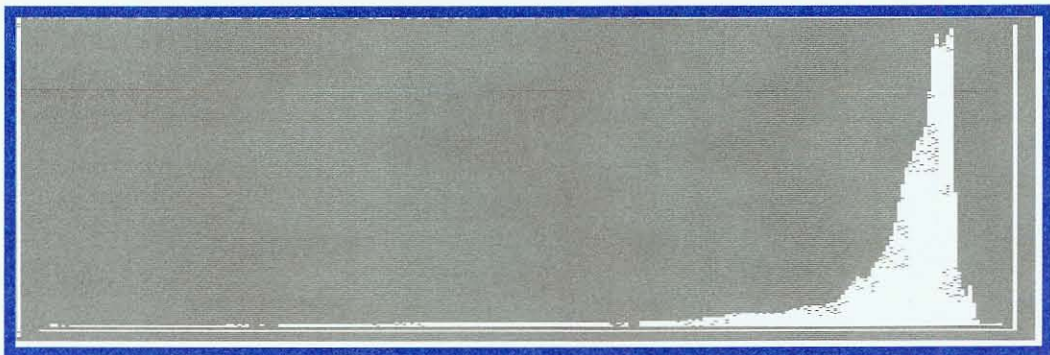
Figure 26: 8-bit Histogram

39

Fig 27: 16-bit single peak not enhanced
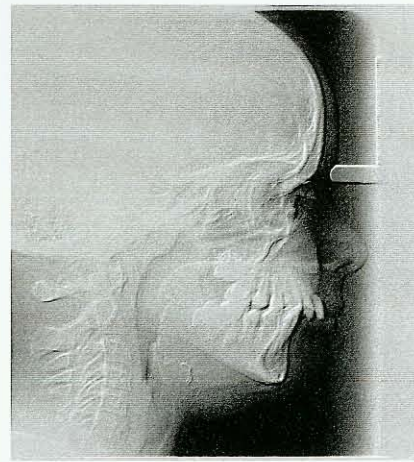
Fig 28: 16-bit single peak emboss
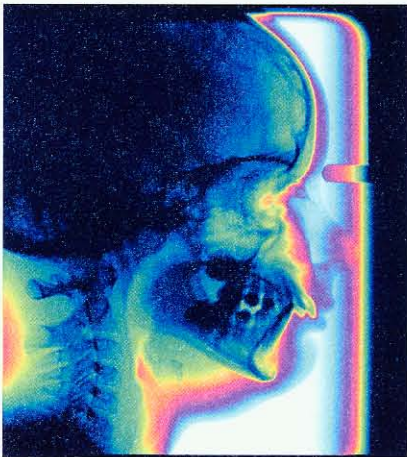
Fig 29: 16-bit single peak colorized
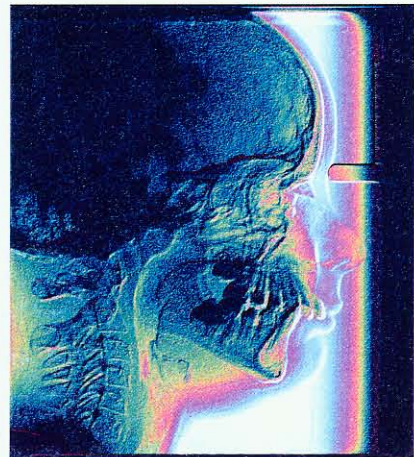
Fig 30: 16-bit single peak emboss/colorized

Figure 31: 16-bit Single Peak Histogram

Fig 32: 16-bit double peak not enhanced
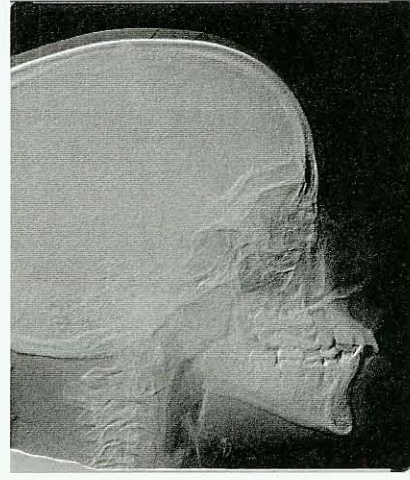
Fig 33: 16-bit double peak emboss
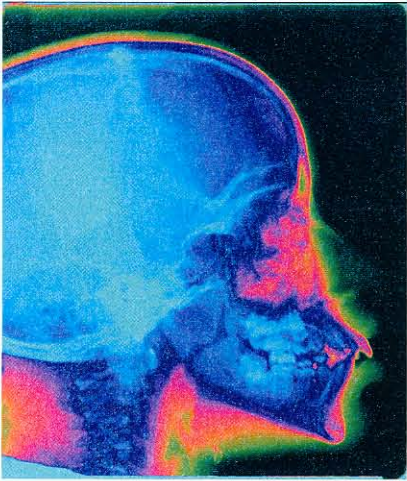
Fig 34: 16-bit double peak colorized
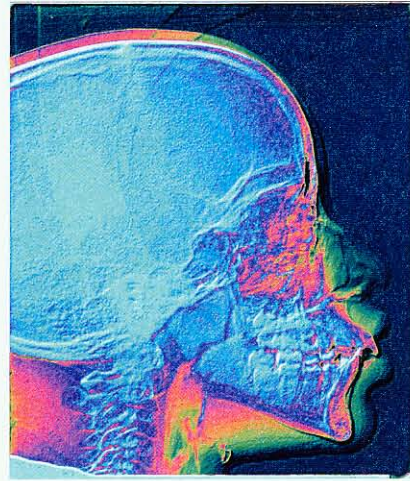
Fig 35: 16-bit double peak emboss/colorized
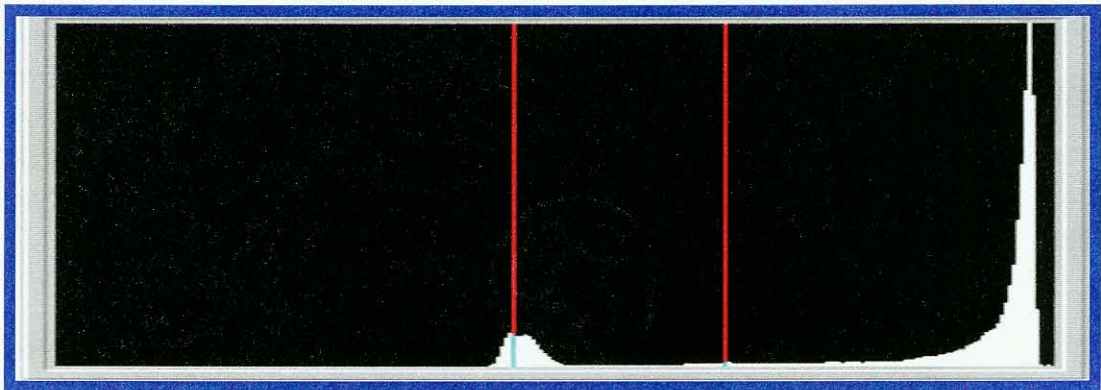
Fig 36: Histogram of 16-bit double peak image

Statistical Analytics

Non-parametric statistical analysis was used to compare differences between the original images and the three selected enhancements for each image. SPSS for Windows, Release 11.0 (SPSS, Chicago, IL) was the statistics software used to analyze the collected data. A non-parametric Freidman analysis utilizing K-related samples was used to determine if a difference existed in ratings detection of the anatomic landmarks and the overall image of the three histograms when the non-enhanced and the three enhanced post-processed images were displayed. If a difference was found, a two-samples related non-parametric post-hoc Wilcoxon test was performed to distinguish the differences among the histograms respective of the individual landmarks and post-processed enhancements. Significance Level was set at $p \leq 0.05$. Rater reliability analysis was performed using statistical percentage agreement among each rater for repeated measures. For Intra-rater reliability, ratings of two or three were considered to be in agreement.

The goal of the statistical analyses was to determine if significant differences exist between the accuracy of cephalometric landmark identification and in preference for overall cephalogram quality using the three selected image enhancements among the three levels of histogram presentation and bit depth. The statistical results and methods are further discussed in Chapters 4 and 5.

Chapter IV

Results

Results for the study include (1) data for each individual landmark and also for the overall image; (2) inter-rater agreement assessment; and (3) intra-rater reliability assessment. The results are presented according to landmark.

Sella

Regarding inter-rater agreement, 8-bit non-enhanced images were preferred to 16-bit single peak and 16-bit double peak non-enhanced images. Emboss/colorized images of all bit depths were preferred over their original counterparts ($p=0.001$, $p=0.001$, $p=0.004$ respectively). Embossed enhancements were significantly preferred over original images for 8-bit and 16-bit single peak images ($p=0.001$; $p=0.001$ respectively). Both simple emboss and emboss/colorized enhancements were preferred over color enhancements for 16-bit single peak images ($p=0.001$; $p=0.003$ respectively).

A summation of raw data points can be found in Tables 4. Acronyms used in Tables 4: PL8 – 8-bit no enhancement, PLE8- 8-bit emboss, IN8 – 8-bit colorized, INE8 –8-bit emboss/colorized; PL161-16-bit single peak no enhancement, PLE-161- 16-bit single peak emboss, IN161-16-bit single peak colorized, INE161-16-bit single peak emboss/colorized; PL162 – 16-bit double peak no enhancement, PLE162 – 16-bit double peak emboss, IN162 – 16-bit double peak colorized, INE162- 16-bit double peak emboss/colorized.

Table 4. Summary of Data Points for Detection of Landmark Sella

PL8	PLE8	IN8	INE8
7	12	11	12
8	11	11	12
8	12	12	12
7	10	10	11
9	10	12	10
8	11	10	12
6	11	11	12
8	12	10	12
7	11	11	10
8	12	12	12

PL161	PLE161	IN161	INE161
5	11	5	11
7	8	5	9
7	12	8	11
4	9	7	8
8	10	5	10
4	9	8	7
6	9	5	10
4	12	6	11
5	9	5	9
6	10	5	11

PL162	PLE162	IN162	INE162
8	8	8	10
6	9	7	9
8	9	10	10
7	6	7	8
6	10	8	6
10	6	7	10
7	8	9	8
8	9	8	11
7	9	8	9
7	9	7	9

Appendix A provides the raw data for all individual data points collected for the

landmark Sella.

44

Percentage agreements among raters and for repeat measures are shown in Table 5.

Table 5. Percentage agreement for repeat measures (Sella)

Image Histogram	Image Enhancement	Intra-rater Agreement (%)	Inter-rater Agreement (%)
8-bit	No enhancement	100	70
	Emboss	100	80
	Color	100	80
	Emboss/Color	100	88
16-bit single peak	No enhancement	40	60
	Emboss	100	58
	Color	80	68
	Emboss/Color	60	68
16-bit double peak	No enhancement	100	48
	Emboss	100	63
	Color	10	60
	Emboss/Color	90	70

Nasion

For inter-rater agreement 16-bit single peak non-enhanced images were preferred to 8-bit and 16-bit double peak non-enhanced images. Emboss images for 16-bit single peak and double peak were preferred over color enhancements ($p=0.004$; $p=0.002$ respectively). The original images for 16-bit single peak and double peak were preferred over color enhancements ($p=0.012$; $p=0.012$). A summation of raw data points for Nasion can be found in the Table 6.

Table 6. Summary of Data Points for Detection of Landmark Nasion

PL8	PLE8	IN8	INE8
10	11	11	10
11	11	9	9
11	11	12	9
7	11	5	11
9	10	11	7
9	9	7	9
8	8	11	6
12	11	11	12
11	11	11	10
10	11	11	10

PL161	PLE161	IN161	INE161
8	10	8	9
10	8	7	10
11	10	7	10
8	8	8	6
10	8	6	9
8	9	7	6
10	8	7	10
9	10	10	8
9	10	7	9
9	10	7	11

PL162	PLE162	IN162	INE162
9	7	6	8
9	9	6	8
9	12	10	8
10	7	5	10
8	10	7	5
9	6	6	9
7	11	8	7
11	10	7	10
8	10	5	8
7	9	6	8

Appendix A lists all individual data points collected for the landmark Nasion.

Percentage agreements among raters and for repeat measures are shown in Table 7.

Table 7. Percentage agreement for repeat measures (Nasion)

Image Histogram	Image Enhancement	Intra-rater Agreement (%)	Inter-rater Agreement (%)
8-bit	No enhancement	90	70
	Emboss	100	65
	Color	80	75
	Emboss/Color	90	70
16-bit single peak	No enhancement	80	75
	Emboss	100	68
	Color	90	65
	Emboss/Color	60	65
16-bit double peak	No enhancement	90	63
	Emboss	100	60
	Color	70	75
	Emboss/Color	90	65

<u>Porion</u>

Regarding inter-rater agreement 16-bit single peak non-enhanced histograms were preferred. Emboss enhancements of 8-bit and 16-bit single peak images were preferred to their original images (p=0.004; p=0.004 respectively). For 8-bit and 16-bit single peak images, emboss/color was preferred over the original images (p=0.009; p=0.001 respectively). Emboss/color was also preferred over emboss and color enhancements for 16-bit single peak images (p=0.047; p=0.002 respectively). Emboss enhancements for 16-bit single peak images were preferred over color enhancement (p=0.012). A summation of raw data points for Porion can be found in the Table 8.

.

Table 8. Summary of Data Points for Detection of Landmark Porion

PL8	PLE8	IN8	INE8
6	6	7	7
6	8	5	10
6	8	7	7
6	6	6	9
6	7	10	4
7	10	4	11
6	7	6	8
6	9	5	10
7	8	8	8
6	9	7	11

PL161	PLE161	IN161	INE161
5	8	5	9
5	5	4	9
4	7	4	9
4	5	4	7
7	9	7	7
7	5	4	7
5	6	6	8
4	8	5	7
5	8	6	7
4	6	4	8

PL162	PLE162	IN162	INE162
5	7	4	11
4	5	6	8
4	7	4	9
7	6	6	7
9	8	4	8
4	6	6	6
6	5	4	8
5	8	4	7
7	8	4	7
6	7	5	8

Appendix A lists all individual data points collected for the landmark Porion.

Percentage agreements among raters and with repeat measures are shown in Table 9.

Table 9. Percentage agreement for repeat measures (Porion)

Image Histogram	Image Enhancement	Intra-rater Agreement (%)	Inter-rater Agreement (%)
8-bit	No enhancement	90	85
	Emboss	60	55
	Color	50	60
	Emboss/Color	70	53
16-bit single peak	No enhancement	70	93
	Emboss	60	63
	Color	80	85
	Emboss/Color	60	65
16-bit double peak	No enhancement	80	60
	Emboss	30	70
	Color	40	73
	Emboss/Color	60	58

<u>Orbitale</u>

Regarding inter-rater agreement, 8-bit histogram images and 16-bit single peak non-enhanced images were equally preferred. For 8-bit and 16-bit single peak images, emboss/color was preferred over the original images ($p=0.005$; $p=0.007$ respectively). Color enhancement for 8-bit images was preferred over original images ($p=0.039$). Emboss/color enhancement for 8-bit images was preferred over emboss images ($p=0.005$). For 16-bit single peak images, emboss was preferred over original images ($p=0.021$). A summation of raw data points can be found in Table 10.

Table 10. Summary of Data Points for Detection of Landmark Orbitale.

PL8	PLE8	IN8	INE8
11	10	9	8
10	9	8	10
12	11	9	9
9	9	6	8
10	10	10	5
10	9	7	8
9	9	11	6
12	12	8	10
10	11	10	8
10	10	10	9

PL161	PLE161	IN161	INE161
8	8	7	9
9	8	9	8
12	10	11	11
7	9	8	6
11	8	9	10
9	7	10	6
9	8	7	8
12	9	12	8
11	8	10	8
10	8	10	8

PL162	PLE162	IN162	INE162
8	9	8	8
9	7	9	5
10	8	8	8
8	7	7	8
9	10	8	6
8	6	8	10
6	9	9	6
12	10	10	11
7	8	8	7
8	8	8	6

Appendix A lists all individual data points collected for the landmark Orbitale.

Percentage agreements among raters and with repeat measures are shown in

Table 11.

Table 11. Percentage agreement for repeat measures (Orbitale).

Image Histogram	Image Enhancement	Intra-rater Agreement (%)	Inter-rater Agreement (%)
8-bit	No enhancement	100	68
	Emboss	100	70
	Color	80	55
	Emboss/Color	60	60
16-bit single peak	No enhancement	90	68
	Emboss	100	68
	Color	100	65
	Emboss/Color	80	65
16-bit double peak	No enhancement	100	63
	Emboss	100	73
	Color	70	68
	Emboss/Color	90	55

<u>Point "A" (Pt. A)</u>

For inter-rater agreement 16-bit single peak non-enhanced histograms were

preferred to 8-bit and 16-bit double peak non-enhanced histograms. For 16-bit single

and double peak images, original images were preferred over color enhancement

($p=0.001$; $p=0.004$ respectively). Emboss was preferred over color for 16-bit single and

double peak images ($p=0.002$; $p=0.001$ respectively). Emboss/color was preferred over

color for 16-bit single peak images ($p=0.022$). Original images and emboss enhancement

for 16-bit double peak were preferred to emboss/color ($p=0.078$; $p=0.066$ respectively).

Emboss enhancement was preferred over original for 16-bit double peak images

($p=0.021$). A summation of raw data points can be found in Table 12.

Table 12. Summary of Data Points for Detection of Landmark Pt. A.

PL8	**PLE8**	**IN8**	**INE8**
9	11	12	7
10	10	8	10
11	11	12	7
8	10	8	9
11	10	10	7
9	11	9	11
9	10	11	5
10	11	8	9
9	8	11	8
10	12	10	10

PL161	**PLE161**	**IN161**	**INE161**
10	11	5	11
11	11	8	9
12	11	11	12
10	11	8	7
12	12	9	12
11	12	10	11
12	10	5	11
12	12	10	8
11	12	6	11
12	12	8	11

PL162	**PLE162**	**IN162**	**INE162**
10	11	8	10
10	12	7	9
11	12	10	9
11	11	6	11
10	12	10	8
11	11	9	12
10	11	9	5
12	12	8	10
9	12	6	8
10	12	10	11

Appendix A lists all individual data points collected for the landmark Pt. A.

Percentage agreements among raters and with repeat measures are shown in Table 13.

Table 13. Percentage agreement for repeat measures (Pt. A).

Image Histogram	Image Enhancement	Intra-rater Agreement (%)	Inter-rater Agreement (%)
8-bit	No enhancement	100	65
	Emboss	100	70
	Color	80	58
	Emboss/Color	70	63
16-bit single peak	No enhancement	100	83
	Emboss	100	88
	Color	80	58
	Emboss/Color	100	68
16-bit double peak	No enhancement	90	78
	Emboss	100	90
	Color	20	43
	Emboss/Color	70	55

Point "B" (Pt. B)

For inter-rater agreement all bit depths were preferred equally. Original

images were preferred over color enhancement for 8-bit, 16-bit single peak, and

16-bit double peak (p=0.008, p=0.008, p=0.031 respectively). Emboss was also

preferred over color for all bit depths (p=0.016, p=0.008, p=0.031 respectively).

A summation of raw data points can be found in Table 14.

Table 14. Summary of Data Points for Detection of Landmark Pt. B.

PL8	PLE8	IN8	INE8
12	12	12	10
12	12	10	12
12	12	12	12
12	12	9	12
12	11	10	12
12	12	11	12
12	11	11	11
12	12	10	12
12	12	12	11
12	12	11	12
PL161	**PLE161**	**IN161**	**INE161**
12	11	9	12
12	12	11	12
12	12	12	12
12	12	11	10
12	12	12	12
12	12	12	11
12	12	9	12
12	12	11	12
12	12	11	12
12	12	11	11
PL162	**PLE162**	**IN162**	**INE162**
12	12	10	11
12	12	12	12
12	12	12	10
12	12	9	12
12	12	12	12
12	12	11	12
12	12	12	12
12	12	12	12
12	12	10	12
12	12	8	12

Appendix A lists all individual data points collected for the landmark Pt. B.

54

Percentage agreements among raters and with repeat measures are shown in Table 15.

Table 15. Percentage agreement for repeat measures (Pt. B).

Image Histogram	Image Enhancement	Intra-rater Agreement (%)	Inter-rater Agreement (%)
8-bit	No enhancement	100	100
	Emboss	100	95
	Color	90	73
	Emboss/Color	100	90
16-bit single peak	No enhancement	100	100
	Emboss	100	98
	Color	90	78
	Emboss/Color	100	90
16-bit double peak	No enhancement	100	100
	Emboss	100	100
	Color	90	80
	Emboss/Color	100	93

Pogonion

For inter-rater agreement all bit depths were preferred equally. There was no particular image type preferred for 8-bit, 16-bit single peak, and 16-bit double peak images. A summation of raw data points can be found in Table 16.

Table 16. Summary of Data Points for Detection of Landmark Pogonion.

PL8	PLE8	IN8	INE8
12	12	12	11
12	12	11	12
12	12	12	12
12	12	12	12
12	12	12	12
12	12	12	12
12	12	11	11
12	12	11	12
12	12	12	11
12	12	12	12

PL161	PLE161	IN161	INE161
12	12	10	12
12	12	12	12
12	12	12	12
12	12	12	12
12	12	12	12
12	12	12	12
12	12	10	12
12	12	12	12
12	12	12	12
12	12	11	12

PL162	PLE162	IN162	INE162
12	12	12	12
12	12	12	12
12	12	12	11
12	12	11	12
12	12	12	12
12	12	12	12
12	12	12	12
12	12	12	12
12	12	11	12
12	12	10	12

Appendix A lists all individual data points collected for the landmark Pogonion.

Percentage agreement among raters and with repeat measures is shown in Table 17.

Table 17. Percentage agreement for repeat measures (Pogonion).

Image Histogram	Image Enhancement	Intra-rater Agreement (%)	Inter-rater Agreement (%)
8-bit	No enhancement	100	100
	Emboss	100	100
	Color	100	93
	Emboss/Color	100	93
16-bit single peak	No enhancement	100	100
	Emboss	100	100
	Color	100	88
	Emboss/Color	100	100
16-bit double peak	No enhancement	100	100
	Emboss	100	100
	Color	100	90
	Emboss/Color	100	98

Pronasale

Inter-rater agreement was greatest for the 16-bit single peak histograms in comparison to 8-bit and 16-bit double peak histograms. For 8-bit and 16-bit double peak images, emboss was preferred over original images ($p=0.001$; $p=0.004$ respectively). Emboss was preferred over color for 8-bit images ($p=0.004$). Emboss/color was preferred over original images for 8-bit and 16-bit double peak images ($p=0.072$, $p=0.004$ respectively). For 16-bit single peak images original was preferred over emboss, color, and emboss/color ($p=0.001$, $p=0.001$, $p=0.035$ respectively). Emboss/color enhancement was preferred over emboss for 16-bit single peak images ($p=0.016$). Color enhancement was preferred over original and emboss for 16-bit double peak images ($p=0.001$, $p=0.023$ respectively). A summation of raw data points can be found in the following table. A summation of raw data points can be found in Table 18.

Table 18. Summary of Data Points for Detection of Landmark Pronasale.

PL8	PLE8	IN8	INE8
10	12	10	9
10	12	10	12
10	11	11	9
7	10	8	11
10	11	11	8
7	12	6	12
9	10	9	10
9	12	8	11
10	12	10	11
8	12	9	12

PL161	PLE161	IN161	INE161
6	4	4	4
6	4	4	5
6	4	4	5
6	4	5	4
8	5	4	6
6	5	4	5
6	4	5	8
6	4	4	5
6	4	5	4
6	4	4	5

PL162	PLE162	IN162	INE162
5	8	12	10
6	10	11	11
9	12	11	9
8	9	9	10
5	10	10	9
7	6	11	12
7	10	10	7
7	8	11	12
7	9	12	12
4	6	10	11

Appendix A lists all individual data points collected for the landmark Pronasale.

Percentage agreements among raters and with repeat measures are shown in Table 19.

Table 19. Percentage agreement for repeat measures (Pronasale).

Image Histogram	Image Enhancement	Intra-rater Agreement (%)	Inter-rater Agreement (%)
8-bit	No enhancement	80	83
	Emboss	100	90
	Color	80	63
	Emboss/Color	100	70
16-bit single peak	No enhancement	100	98
	Emboss	100	95
	Color	100	95
	Emboss/Color	70	75
16-bit double peak	No enhancement	90	73
	Emboss	100	60
	Color	90	78
	Emboss/Color	100	68

<u>Labrale Superius</u>

Regarding inter-rater agreement, 16-bit single peak non-enhanced images were preferred in comparison to 8-bit and 16-bit double peak non-enhanced images. For 16-bit single and double peak images, color was preferred over original images ($p=0.031$; $p=0.004$ respectively). Color was preferred over emboss for 16-bit single and double peak images ($p=0.006$, $p=0.010$ respectively). Emboss/color was preferred over emboss for 16-bit single peak images and over original images for 16-bit double peak images ($p=0.023$, $p=0.006$ respectively). Emboss was preferred over original images for 16-bit single peak images ($p=0.01$). A summation of raw data points can be found in Table 20.

Table 20. Data Points for Detection of Landmark Labrale Superius.

PL8	PLE8	IN8	INE8
9	8	12	9
9	10	8	10
11	11	11	9
6	11	7	11
9	9	11	8
9	10	8	12
8	10	10	8
10	12	12	11
10	9	12	8
8	10	10	11

PL161	PLE161	IN161	INE161
6	4	11	6
7	5	11	9
9	11	11	11
6	5	8	5
9	8	7	10
7	5	10	5
8	5	6	7
7	8	10	9
7	8	10	7
7	6	8	9

PL162	PLE162	IN162	INE162
7	10	12	12
8	10	12	12
11	12	11	10
8	11	11	10
8	11	12	10
9	9	11	12
9	10	11	9
11	10	11	12
10	10	12	12
7	10	12	12

Appendix A lists all individual data points collected for the landmark Labrale Superius.

Percentage agreements among raters and with repeat measures are shown in Table 21.

Table 21. Percentage agreement for repeat measures (Labrale Superius).

Image Histogram	Image Enhancement	Intra-rater Agreement (%)	Inter-rater Agreement (%)
8-bit	No enhancement	100	68
	Emboss	100	70
	Color	100	55
	Emboss/Color	100	68
16-bit single peak	No enhancement	40	73
	Emboss	60	60
	Color	90	48
	Emboss/Color	80	58
16-bit double peak	No enhancement	80	53
	Emboss	100	80
	Color	90	88
	Emboss/Color	100	78

Labrale Inferius

For inter-rater agreement 16-bit single peak non-enhanced images were preferred to 8-bit images and 16-bit double peak histogram images. Color was preferred over original images for 16-bit single and double peak images (p=0.020, p=0.012 respectively). Color was also preferred over emboss for both 16-bit single and double peak images (p=0.010, p=0.027 respectively). For 16-bit single peak images, emboss color was preferred over emboss while emboss/color was preferred over original images for 16-bit double peak images (p=0.016, p=0.027 respectively). A summation of raw data points can be found in Table 22.

Table 22. Summary of Data Points for Detection of Landmark Labrale Inferius.

PL8	PLE8	IN8	INE8
9	7	12	9
10	10	8	10
11	11	11	9
7	9	9	11
9	9	12	8
9	10	8	12
8	10	10	8
10	11	12	12
9	9	11	9
8	9	10	11

PL161	PLE161	IN161	INE161
6	4	11	6
7	7	11	9
11	11	11	11
6	6	8	6
9	9	7	10
7	5	10	6
8	5	8	8
8	9	11	9
7	8	10	8
7	6	9	10

PL162	PLE162	IN162	INE162
7	10	12	12
10	11	12	12
11	12	11	10
9	11	11	10
8	11	12	10
10	9	11	12
9	10	11	9
11	11	11	12
10	11	12	12
7	10	12	12

Appendix A lists all individual data points collected for the landmark Labrale Inferius.

Percentage agreements among raters and with repeat measures are shown in Table 23.

Table 23. Percentage agreement for repeat measures (Labrale Inferius)

Image Histogram	Image Enhancement	Intra-rater Agreement (%)	Inter-rater Agreement (%)
8-bit	No enhancement	90	68
	Emboss	100	63
	Color	100	58
	Emboss/Color	100	68
16-bit single peak	No enhancement	40	70
	Emboss	80	50
	Color	90	55
	Emboss/Color	100	48
16-bit double peak	No enhancement	90	60
	Emboss	70	63
	Color	90	88
	Emboss/Color	100	78

Soft Tissue Pogonion

Regarding inter-rater agreement, 16-bit single peak non-enhanced images were preferred to 8-bit and 16-bit double peak non-enhanced histograms. Color enhancement was preferred over original images for all bit-depths ($p=0.016$, $p=0.008$, $p=0.008$ respectively). Color enhancement was preferred over emboss enhancement for all bit depths ($p=0.045$, $p=0.008$, $p=0.023$ respectively). Emboss/color was preferred over emboss for 8-bit and 16-bit single peak images ($p=0.016$, $p=0.008$ respectively). Emboss/color was preferred over original images for 16-bit single and double peak images ($p=0.031$, $p=0.023$ respectively). A summation of raw data points can be found in Table 24

Table 24. Summary of Data Points for Detection of Landmark Soft Tissue Pogonion

PL8	PLE8	IN8	INE8
10	7	12	9
11	8	11	12
11	12	11	11
8	10	9	11
10	8	12	8
8	9	8	12
10	10	10	10
11	11	12	12
11	9	12	11
8	9	11	12

PL161	PLE161	IN161	INE161
8	6	12	9
10	8	12	10
11	11	11	11
9	7	9	9
9	10	10	10
9	7	11	9
9	7	9	11
9	11	11	11
9	9	12	10
10	8	12	10

PL162	PLE162	IN162	INE162
7	10	12	11
10	10	12	12
11	12	11	10
9	11	11	10
9	10	12	10
11	10	11	12
10	10	11	10
11	11	11	12
11	10	12	11
8	11	12	12
7	10	12	11

Appendix A lists all individual data points collected for the landmark.

Percentage agreements among raters and with repeat measures are shown in Table 25.

Table 25. Percentage agreement for repeat measures (Soft Tissue Pogonion)

Image Histogram	Image Enhancement	Intra-rater Agreement (%)	Inter-rater Agreement (%)
8-bit	No enhancement	100	70
	Emboss	100	58
	Color	100	73
	Emboss/Color	100	70
16-bit single peak	No enhancement	100	83
	Emboss	80	63
	Color	100	73
	Emboss/Color	100	70
16-bit double peak	No enhancement	80	68
	Emboss	100	88
	Color	90	88
	Emboss/Color	100	80

Perceived Overall Image Quality

Regarding inter-rater agreement, 16-bit single peak non-enhanced images were preferred to 8-bit and 16-bit double peak non-enhanced histograms. There were no significant differences found for 8-bit images. Emboss/color enhancement was preferred over original images for both 16-bit depths (p=0.016, p=0.002 respectively). Emboss/color enhancement was preferred over color enhancement for both 16-bit single and double peak images (p=0.039, p=0.022 respectively). Emboss was preferred over original images for 16-bit double peak images (p=0.016). A summation of raw data points can be found in Table 26.

Table 26. Summary of Data Points for Detection of Overall Quality

PL8	PLE8	IN8	INE8
7	8	10	8
7	8	5	10
8	11	9	8
5	9	5	11
9	10	9	8
9	8	7	9
8	8	9	7
9	11	7	11
7	10	11	8
7	10	9	10

PL161	PLE161	IN161	INE161
5	4	5	9
5	4	4	5
6	7	7	8
4	6	6	4
7	8	8	8
8	8	8	8
6	5	5	8
7	7	6	8
4	6	4	6
8	7	4	8

PL162	PLE162	IN162	INE162
5	7	5	9
4	6	7	8
8	8	8	9
7	7	7	9
7	10	8	9
8	7	8	10
6	9	8	7
8	8	7	10
6	8	5	6
5	8	8	7
5	7	5	9

Appendix A lists all individual data points collected for the perceived Overall Image Quality.

Percentage agreements among raters and with repeat measures are shown in Table 27.

Table 27. Percentage agreement for repeat measures (Overall Image Quality).

Image Histogram	Image Enhancement	Intra-rater Agreement (%)	Inter-rater Agreement (%)
8-bit	No enhancement	90	65
	Emboss	90	68
	Color	70	58
	Emboss/Color	70	68
16-bit single peak	No enhancement	60	70
	Emboss	70	65
	Color	80	55
	Emboss/Color	50	65
16-bit double peak	No enhancement	60	60
	Emboss	90	70
	Color	80	63
	Emboss/Color	90	75

Summary of Results

In detection of hard tissue landmarks: For landmark Sella 8-bit histograms were preferred. Emboss images for all bit depths were preferred over other enhancements applied.

Raters favored 16-bit double peak histograms over 16-bit single peak histograms when identifying Nasion. Non-enhanced and emboss images for both 16-bit histograms were preferred over color enhancement.

For landmark Porion 8-bit histograms were preferred over 16-bit single peak histograms. Emboss and emboss/color enhancements were favored over non-enhanced images for both 8-bit and 16-bit single peak histograms.

Raters favored 8-bit histograms over 16-bit single peak histograms when identifying Orbitale. Color and emboss/color enhancements were preferred to non-enhanced images for 8-bit histograms. For 16-bit single peak histograms emboss and emboss/color enhancements were preferred to non-enhanced images.

For landmark Point "A" (Pt A) 16-bit double peak histograms were preferred over 16-bit single peak histograms. Emboss enhancement was favored over non-enhanced images 16-bit double peak histograms.

For landmark Point "B" (Pt B) both 8-bit and 16-bit double peak histograms were preferred over 16-bit single peak histograms. Non-enhanced and emboss images were equally preferred over color enhancement for all bit depths.

No significant differences were reported for the identification of landmark Pogonion.

In detection of Soft Tissue Landmarks: For landmark Pronasale Raters favored both 8-bit and 16-bit double peak histograms over 16-bit single peak histograms. Emboss and emboss/color enhancements were favored over non-enhanced 8-bit histograms. Non-enhanced images were preferred to enhanced images for 16-bit single peak images. All three enhancements were preferred over non-enhanced images for 16-bit double peak images.

Raters favored 16-bit double peak histograms over 16-bit single peak histograms when identifying Labrale Superius. Color and emboss/color enhancements were preferred

to non-enhanced images for 16-bit single peak histograms. For 16-bit double peak histograms emboss, color and emboss/color enhancements were preferred to non-enhanced images.

Raters favored 16-bit double peak histograms over 16-bit single peak histograms when identifying Labrale Inferius. Color and emboss/color enhancements were preferred to non-enhanced images for 16-bit single peak histograms. For 16-bit double peak histograms emboss, color and emboss/color enhancements were preferred to non-enhanced images.

For landmark Soft Tissue Pogonion 16-bit double peak histograms were preferred over 16-bit single peak histograms. Color and emboss/color enhancements were favored over non-enhanced images for all bit depths.

Perceived Overall Image Quality: Raters preferred 16-bit double peak histograms. Emboss/color enhancement was favored for 16-bit single peak histograms. Emboss and emboss/color enhancements were favored for 16-bit double peak histograms.

Chapter V

Discussion

Three measurements were taken from the statistical analysis of this study's data. These measurements consist of Inter-rater percentage agreement, Intra-rater reliability, and a combination of Friedman analysis of variance and Wilcoxon post-hoc analysis to determine statistically significant differences. The first measurement acquired was the Inter-rater percentage agreement revealing images preference among all ten raters. It should be noted that there was never 100% agreement among raters and percentages ranged from 43%-98%. Overall inter-rater percentage agreement was moderate. Rater reliability analysis was performed using statistical percentage agreement among the raters' repeated measures. This revealed higher percentages of agreement within individual raters than between raters. Overall intra-rater reliability was high. The previous literature states that a major error with cephalometric radiology is uncertainty between and among observer's identification of radiographic landmarks. The wide range of inter-rater agreement percentages and varying intra-rater reliability presented in this study supports this statement.

Previous studies by West at the University of Louisville found that the overall images resulted in rating differences based on histogram presentation and enhancements applied. In all cases 8-bit and 16-bit double peak images were favored to 16-bit single

peak histogram images.[6] The current study supports this conclusion with either 8-bit or 16-bit double peak images being preferred to 16-bit single peak images in all cases.

Regarding image enhancement, raters preferred enhanced images over non-enhanced images a majority of the time. Of the twelve categories (eleven landmarks and overall image quality) rated, nine were preferred with the use of enhancement. There appeared to be a trend toward a preference for the emboss enhancement of hard tissue landmarks and color enhancement for soft-tissue landmarks.

Raters preferred color enhancement for detecting Labrale Superius and Labrale Inferius during the current investigation. Similar inquiries about color enhancement techniques previously have been made concerning periodontal lesions. In 1991, Reddy supported the idea that pseudocolor enhancement combined with digital subtraction radiography may be a significant aid to the average clinician in the detection of periodontal lesions.[43] In 1999, at the University of Louisville School of Dentistry it was concluded color-coded image processing of digital images had limited value in the estimation of peri-radicular lesional dimensions.[44] Likewise the present study suggests additional benefits using color enhancement of digital images in orthodontics where subtle soft tissue landmarks are concerned. The current study results definitely warrant further investigations into the possible benefits of color and emboss enhancement techniques for cephalometric landmark detection. Cephalometric radiography could potentially also benefit from using digital enhancement techniques to detect unsuspected pathologic lesions.

Chapter VI

Conclusions

The results support the use of emboss and color enhancements to aid in the quality

of landmark identification and improved perception of image quality for photostimuable

phosphor cephalograms. Emboss enhancement seems to be best utilized for hard tissue

landmarks while color enhancement seems to be best utilized for soft-tissue landmarks.

CHAPTER VII

Suggestions for Future Research

Using the same group of images as used in this study, further investigations might include:

1) Allowing raters to control contrast and brightness (window and leveling). This was not possible under the simultaneous viewing design employed in the present study. This would permit "optimum" viewing by the individual raters.

2) Allowing raters to control color enhancement of each image. The present viewing software VixWin 2000© uses a spectrum or sliding algorithm to colorize images. In this study the presenter determined the colorization of each image. Rater control over color enhancement was not feasible under the simultaneous viewing design employed in the present study.

3) Utilization of additional post-processing software and enhancement algorithms to view the same images.

4) Analysis of images for detection of oral pathologic lesions rather than normal landmarks utilizing the selected post-processing image enhancements.

References

1. Broadbent BH. A new x-ray technique and its application to orthodontia. Angle Orthod 1931;1:45-66.
2. Athanasiou A.E., Orthodontic Cephalometry. Mosby-Wolfe 1995.
3. Sonoda M, Takeno M, Miyahara J, Kato H, Computed Radiography utilizing scanning laser stimulated luminescence. Radiol 1983;148:833-838.
4. Cowen AR, Workman A, Price JS. Physical aspects of photostimulable phosphor computed radiography. Br J Radiol 1993; 66:332-345.
5. Tateno Y, Iinuma TA, Takano, Computed Radiography, Springer-Verlag, 1987.
6. West KD. Post-processing contrast enhancements in 8-bit and 16-bit photostimuable phosphor cephalograms. Masters Thesis, University of Louisville Graduate School, May 2003.
7. Takahashi K, Kohda K, Miyahara J, Kanemitsu Y, Amitanik K, Shionoya S. Mechanism of photostimulated luminescence in $BaFX;Eu^{2+}$ (X = Cl, Br) phosphors. J Lumin 1984; 31/32:266-268.
8. Huda W, Rill N, Benn K, Pettigrew C. Comparison of a photostimulable phosphor system with film for dental radiology. Oral Surg Oral Med Oral Path Oral Radiol Endod 1997;83:725-31.
9. Kato, H., Miyahara, J., Takano, M., New computed radiography using scanning laser stimulated luminescence. Neurosurg Rev 1985; 8:53-62.
10. Characteristic Curve, Medcyclopaedia – The complete online version of the Encyclopedia of Medical Imaging by NICER. www.amershamhealth.com
11. Vickers SE, West KD, Silveira AM, Johnson BE, Farman AG. Image enhancement outcomes for 8-bit and 16-bit photostimulable phosphor cephalograms. American Association of Orthodontists Annual Session, 2002.
12. Goaz PW, White SC. Oral Radiology, 2nd ed. Mosby Co 1987.
13. White SC, Pharoah MJ, Oral Radiology, Principles and Interpretation, 4th ed. Mosby Co 2000.
14. Dahlberg G. Statistical methods for medical and biological students. Interscience Publications 1940.
15. Kogutt MS, Jones JP, Perkins DD. Low-dose digital computed radiography in pediatric chest imaging. Am J Roentgenol. 1988;151:775-779.
16. Seki, K., Okano, T., Exposure reduction in cephalography with a digital photostimulable phosphor imaging system. Dentomaxillofac Radiol Aug 1993; 22:127-130.
17. Lim KF, Foong KW, Phosphor-stimulated Computed Cephalometry: Reliability of Landmark Identification. Br J Orthod Nov 1997; 24:301-308.

18. Naslund EB, Kruger M, Petersson A, Hansen K. Analysis of low-dose digital lateral cephalometric radiographs. Dentomaxillofac Radiol May 1998; 27:136-9.
19. Cohen AM. Uncertainty in cephalometrics. Br J Orthod 1984;11:44-48.
20. Tng T, Chan T, Hagg U, Cooke MS. Validity of cephalometric landmarks. An experimental study on human skulls. Europ J Ortho1994;16:110-120.
21. Hagg U, Cooke MS, Chan C, Tng T, Lau Y. The reproducibility of cephalometric landmarks: an experimental study on skulls. Aust J Ortho 1998; 15:177-185.
22. Thurrow RC. Cephalometric methods in research and private practice. Angle Orthod 1951;21:194-198.
23. Balter S. Fundamental properties of digital images. Radiographics 1993;13:129-141.
24. Farman AG, Scarfe WC. Pixel perception and voxel vision constructs for a new paradigm in maxillofacial imaging. Dentomaxillofac Radiol 1994;23:5-9.
25. Conover GL, Hildebolt CF, Anthony D. A comparison of six intra-oral x-ray films. Dentomaxillofac Radiol 1995;24:169-172.
26. Macri V, Wenzel A. Reliability of landmark recording on film and digital lateral cephalograms. Eur J Orthod 1993;15:137-148.
27. Delgado M. Single versus Twin Peak Histograms: Orthodontic Measurement Accuracy using Photostimulable Phosphor Lateral Cephalograms, Masters Thesis, University of Louisville Graduate School, May 2001.
28. Brettle DS, Workman A, Ellwood RP, Launders JH, Horner K, Davies RM, The imaging performance of a storage phosphor system for dental radiography. Br J Radiol 1996;69:256-261.
29. Stamatakis HC, Welander U, McDavid WD, Physical properties of a photostimulable phosphor system for intra-oral radiography. Dentomaxillofacial Radiology 2000; 29:28-34.
30. Forsythe DB, Shaw WC, Richmond S. Digital imaging of cephalometric radiology. Part I: Advantages and limitation of digital imaging. Angle Orthod 1996; 66:37-42.
31. Borg E, Attaelmanan A, Gröndahl, H-G., Image plate systems differ in physical performance. Oral Surg Oral Med Oral Pathol Oral Radiol Endod 2000; 89:118-124.
32. Wenzel A, Sewerin I. Source of noise in digital subtraction radiography. Oral Surg Oral Med Oral Pathol Oral Radiol Endod 1991;71:503-508.
33. Ishida M, Doi K, Loo LN, Metz CE, Lehn JL. Digital image processing: Effect on detectability of simulated low-contrast radiographic patterns. Radiol 1984;150:569-575.
34. Kvarn E, Krogstad O. Variability in tracings of lateral head plates for diagnostic orthodontic purposes. A methodological study. Acta Odontol Scan 1969;27:359-369.
35. Siegel EL, Reiner BI. Educational exhibit at the 18th Symposium for Computer Applications in Radiology, Salt Lake City, May, 2001.
36. Kawaida M, Fukuda H, Kohno N. Digital Image Processing of Laryngeal Lesions by Electronic Videoendoscopy. Laryngoscope 2002;112:559-564.
37. Bocklage R. Computer analysis of titanium implants in atrophic arch and poor quality bone: a case report. Implant Dent 2001;10:162-167.

38. Menig, J. The DenOptix digital radiographix system. J Clin Orthod 1999;33:407-410

39. Lundström A, Forsberg CM, Westergren H, Lundstrom F. A comparison between estimated and registered natural head position. Eur J Orthod 1991;13:59-64.

40. Crozier S. Is it time yet? Digital x-rays are here to stay, but how do you decide when to switch radiography systems? ADA News June 1999; 28-32.

41. Research Randomizer. www.randomizer.org, 2001.

42. Farman TT, Farman AG. Optimal processing and enhancement of 16-bit photostimulable phosphor images. Radiology 2000;217(P):657.

43. Reddy MS, Bruch JM, Jeffcoat MK, Williams RC. Contrast as an aid to interpretation in digital subtraction radiography. Oral Surg Oral Med Oral Pathol. 1991;71:763-769.

44. Scarfe WC, Czerniejewski VJ, Farman AG, Avant SL, Molteni R. In vivo accuracy and reliability of color-coded image enhancements for the assessment of periradicular lesion dimensions. Oral Surg Oral Med Oral Pathol Oral Radiol Endod 1999;88:603-611.

45. Schaetzing R. Computed Radiography Technology. Advances in Digital Radiography Categorical Course in Diagnostic Radiology Physics (2003 Syllabus).Annual Meeting of the Radiological Society of North America. Nov 2003;7-22.

APPENDICES

Appendix A

Raw Data points for raters:

The following define values: PL8 – 8-bit no enhancement, PLE8- 8-bit emboss, IN8

– 8-bit color, INE8 –8-bit emboss/color; PL161-16-bit single peak no enhancement,

PLE-161- 16-bit single peak emboss, IN161-16-bit single peak color, INE161-16-bit

single peak emboss/color; PL162 – 16-bit double peak no enhancement, PLE162 – 16-

bit double peak emboss, IN162 – 16-bit double peak color, INE162- 16-bit double peak

emboss/color.

Sella:

PL8

3	1	2	1
3	1	2	2
3	1	1	3
3	1	2	1
3	2	1	3
3	1	2	2
2	1	1	2
3	1	1	3
3	1	1	2
3	1	2	2

PLE8

3	3	3	3
3	2	3	3
3	3	3	3
3	3	2	2
3	3	2	2
3	2	3	3
2	3	3	3
3	3	3	3
3	3	3	2
3	3	3	3

IN8

3	3	3	2
2	3	3	3
3	3	3	3
2	3	3	2
3	3	3	3
2	3	3	2
3	3	3	2
3	2	3	2
3	3	3	2
3	3	3	3

INE8

3	3	3	3
3	3	3	3
3	3	3	3
3	3	3	2
2	2	3	3
3	3	3	3
3	3	3	3
3	3	3	3
3	2	3	2
3	3	3	3

PL161

1	2	1	1
2	2	2	1
2	2	1	2
1	1	1	1
2	2	2	2
1	1	1	1
2	2	1	1
1	1	1	1
1	1	1	2
2	1	1	2

PLE161

3	3	2	3
2	2	2	2
3	3	3	3
2	3	2	2
1	3	3	3
3	3	2	1
2	2	3	2
3	3	3	3
2	2	3	2
2	3	3	2

IN161

1	2	1	1
1	2	1	1
2	3	2	1
2	2	2	1
1	1	1	2
2	3	2	1
1	1	1	2
1	3	1	1
1	2	1	1
1	2	1	1

INE161

3	3	3	2
3	2	2	2
3	3	3	2
3	1	2	2
3	3	3	1
2	1	2	2
3	2	2	3
3	3	3	2
3	2	2	2
3	3	3	2

PL162

3	2	2	1
2	1	2	1
3	3	1	1
2	2	2	1
2	1	1	2
3	3	3	1
2	1	2	2
3	2	1	2
1	2	2	2
3	1	1	2

PLE162

2	3	2	1
2	3	2	2
3	2	2	2
2	2	1	1
3	3	2	2
1	2	1	2
2	3	1	2
3	2	2	2
2	3	2	2
2	3	1	3

IN162

1	2	2	3
2	2	1	2
2	3	2	3
1	2	2	2
2	3	2	1
2	1	1	3
2	2	2	3
1	3	1	3
2	2	2	2
2	2	1	2

INE162

3	3	2	2
2	3	2	2
3	3	2	2
2	2	2	2
1	2	1	2
2	3	2	3
2	3	1	2
3	3	2	3
2	3	2	2
2	3	1	3

Repeat Measures:

PL8AA	PLE8BB	IN8CC	INE8DD
3	3	3	3
3	3	3	3
3	3	3	3
3	3	2	2
3	2	2	3
3	3	2	3
3	3	3	3
3	3	3	2
3	2	2	3
3	3	3	3

PL161AA	PLE161BB	IN161CC	INE161DD
2	3	1	2
1	2	2	3
1	3	2	3
1	2	2	1
2	2	1	3
1	3	2	2
1	2	1	1
1	3	1	2
2	2	1	1
1	3	2	2

PL162AA	PLE162BB	IN162CC	INE162DD
3	2	1	3
2	3	2	2
3	3	1	3
2	2	2	2
2	2	1	3
3	3	2	1
2	2	1	2
3	2	2	2
1	2	1	2
3	3	2	2

Nasion

<u>PL8</u>

3	3	2	2
3	3	2	3
3	3	2	3
2	2	2	1
3	3	1	2
3	3	2	1
2	2	1	3
3	3	3	3
3	3	2	3
3	3	2	2

<u>PLE8</u>

2	3	3	3
2	3	3	3
3	3	2	3
3	2	3	3
3	3	2	2
2	2	2	3
2	3	1	2
3	2	3	3
3	3	2	3
3	3	2	3

<u>IN8</u>

3	3	3	2
2	3	2	2
3	3	3	3
1	2	1	1
3	3	3	2
2	1	2	2
3	3	3	2
3	3	3	2
3	3	3	2
3	3	3	2

INE8

2	3	3	2
2	2	3	2
2	2	3	2
2	3	3	3
1	2	3	1
2	2	3	2
1	2	1	2
3	3	3	3
3	2	3	2
2	3	3	2

PL161

3	1	3	1
3	2	3	2
3	2	3	3
3	1	3	1
3	2	3	2
3	1	3	1
3	2	3	2
3	1	3	2
3	1	2	3
3	1	3	2

PLE161

2	3	3	2
2	2	2	2
2	3	3	2
3	2	2	1
1	3	2	2
3	2	2	2
1	2	3	2
2	3	3	2
2	3	3	2
2	3	3	2

IN161

1	3	3	1
1	3	2	1
1	2	3	1
2	3	2	1
1	1	2	2
1	3	2	1
1	1	3	2
2	3	3	2
1	3	2	1
1	2	3	1

INE161

1	3	3	2
2	3	3	2
2	3	3	2
1	1	3	1
2	2	3	2
1	1	3	1
3	2	3	2
1	2	3	2
2	2	3	2
2	3	3	3

PL162

2	2	2	3
2	3	2	2
1	3	2	3
3	2	2	3
1	3	1	3
2	2	2	3
1	2	1	3
3	3	2	3
2	2	1	3
1	2	1	3

PLE162

1	3	2	1
2	3	1	3
3	3	3	3
1	2	2	2
2	3	2	3
1	2	1	2
3	3	2	3
2	3	2	3
2	2	3	3
2	2	2	3

IN162

1	2	1	2
1	2	1	2
2	3	2	3
1	1	1	2
1	3	1	2
1	2	1	2
2	2	2	2
1	2	2	2
1	2	1	1
1	2	1	2

INE162

1	3	2	2
1	3	2	2
1	2	2	3
2	3	2	3
1	1	1	2
2	2	3	2
1	2	2	2
2	3	2	3
2	3	1	2
1	3	2	2

Repeat Measures:

PL8AA	PLE8BB	IN8CC	INE8DD
3	3	3	3
3	3	3	3
3	3	2	3
1	3	2	2
3	2	2	2
3	2	2	3
3	2	1	2
3	3	3	3
3	3	2	2
3	3	3	3

PL161AA	PLE161BB	IN161CC	INE161DD
2	3	3	1
2	3	3	2
3	2	3	2
1	3	3	2
2	2	1	2
1	3	2	2
2	2	2	2
2	3	3	2
2	3	2	2
2	3	3	1

PL162AA	PLE162BB	IN162CC	INE162DD
2	3	1	3
3	3	1	2
2	3	2	3
2	3	2	2
1	2	1	3
2	3	2	1
1	2	1	3
3	3	2	3
2	3	1	2
1	2	2	3

Porion

<u>PL8</u>

3	1	1	1
3	1	1	1
3	1	1	1
3	1	1	1
2	1	1	2
3	1	2	1
2	1	1	2
3	1	1	1
3	1	1	2
3	1	1	1

PLE8

3	1	2	2
2	1	2	3
3	1	2	2
2	1	1	2
3	2	1	1
2	3	2	3
1	2	2	2
3	1	3	2
3	3	1	1
3	1	2	3

IN8

3	2	1	1
2	1	1	1
1	2	2	2
3	1	1	1
3	3	2	2
1	1	1	1
3	1	1	1
2	1	1	1
3	1	2	2
2	1	3	1

INE8

2	2	2	1
3	2	2	3
2	2	2	1
2	2	2	3
1	1	1	1
3	3	2	3
2	3	1	2
2	3	2	3
3	2	1	2
3	3	3	2

PL161

1	1	1	1
1	1	1	1
1	1	1	1
3	1	1	1
1	2	1	1
1	1	1	1
2	1	1	1
1	1	1	1
1	1	1	1
1	1	1	1

PLE161

1	3	2	1
2	1	1	1
2	2	2	1
2	2	1	1
1	3	2	2
2	2	1	1
1	1	1	2
2	2	2	2
2	2	2	2
2	2	2	1

IN161

1	1	1	1
2	2	1	1
1	1	1	1
2	2	1	1
1	1	1	1
1	3	1	1
1	1	1	1
1	1	1	1
1	1	1	1
1	2	1	1

INE161

3	3	3	2
3	2	1	2
3	3	1	2
2	2	1	2
3	2	2	1
1	1	1	3
3	2	1	2
2	2	1	2
3	2	1	1
2	2	1	3

PL162

2	2	1	1
2	1	2	1
1	1	1	1
1	2	1	2
1	2	1	2
3	1	2	1
1	2	2	2
1	1	1	2
1	2	1	1
1	1	1	2

PLE162

1	1	1	1
1	1	1	1
1	2	1	1
1	1	2	1
1	3	2	3
1	1	1	1
1	1	1	2
1	2	1	1
2	1	2	2
2	1	1	2

<u>IN162</u>

1	1	1	1
1	1	1	2
1	1	2	1
1	1	2	2
1	2	2	1
1	1	1	3
1	1	2	2
1	1	1	2
1	1	2	1
1	1	1	1

<u>INE162</u>

2	2	2	2
2	3	2	2
1	2	2	2
1	2	2	2
1	1	1	2
2	3	3	3
1	1	2	1
2	3	2	3
1	2	1	1
1	2	2	1

Repeat Measures:

PL8AA	PLE8BB	IN8CC	INE8DD
1	1	1	2
3	**2**	**1**	**3**
2	1	1	2
2	**2**	**2**	**2**
3	1	1	1
2	**3**	**1**	**3**
2	2	1	2
3	**1**	**1**	**2**
3	1	1	1
3	**1**	**1**	**3**

PL161AA	PLE161BB	IN161CC	INE161DD
1	2	1	3
1	2	1	1
1	2	1	2
1	3	1	2
2	2	1	3
1	3	2	1
1	2	1	2
1	2	1	2
2	1	3	2
1	1	1	2

PL162AA	PLE162BB	IN162CC	INE162DD
2	2	1	3
2	2	2	2
1	1	1	2
2	1	2	2
1	1	1	3
3	2	2	1
1	1	1	2
2	1	1	2
1	2	1	2
1	1	1	2

Orbitale

<u>PL8</u>

3	3	2	3
3	2	2	3
3	3	3	3
3	2	2	2
3	3	1	3
3	2	3	2
3	2	2	2
3	3	3	3
3	2	2	3
3	3	2	2

PLE8

3	3	2	2
2	3	2	2
3	3	2	3
3	2	2	2
3	3	2	2
2	2	3	2
2	2	2	3
3	3	3	3
3	3	3	2
3	3	2	2

IN8

3	2	3	1
2	2	2	2
2	3	3	1
2	1	2	1
3	3	3	1
2	1	3	1
3	3	3	2
2	2	2	2
3	2	3	2
3	3	3	1

INE8

2	2	3	1
2	3	3	2
2	3	2	2
2	2	2	2
1	1	2	1
2	2	2	2
1	3	1	1
2	3	3	2
2	2	2	2
2	3	3	1

PL161

3	2	1	2
3	2	2	2
3	3	3	3
2	1	2	2
3	2	3	3
2	2	3	2
2	2	3	2
3	3	3	3
3	3	3	2
3	2	3	2

PLE161

2	3	2	1
2	2	2	2
2	3	3	2
2	3	1	3
1	3	2	2
3	2	1	1
2	2	2	2
2	3	2	2
2	2	2	2
2	3	1	2

IN161

2	2	2	1
2	3	2	2
3	3	3	2
2	2	2	2
3	2	2	2
3	3	2	2
2	1	2	2
3	3	3	3
3	3	2	2
2	3	3	2

INE161

2	3	3	1
2	2	2	2
3	3	3	2
1	1	2	2
3	3	3	1
1	1	2	2
2	2	2	2
2	2	2	2
2	2	2	2
2	2	2	2

PL162

3	2	1	2
2	3	1	3
2	3	2	3
2	3	1	2
2	3	1	3
3	2	1	2
2	2	1	1
3	3	3	3
2	2	1	2
2	2	1	3

PLE162

2	3	2	2
2	2	1	2
2	2	2	2
2	2	2	1
2	3	2	3
2	1	1	2
2	3	2	2
2	2	3	3
2	2	2	2
2	2	2	2

IN162

2	3	1	2
2	3	1	3
2	2	2	2
2	2	1	2
2	3	1	2
2	2	1	3
3	2	2	2
2	3	2	3
2	3	1	2
2	2	1	3

INE162

1	3	1	3
1	2	1	1
2	3	1	2
2	2	2	2
1	2	1	2
2	3	2	3
1	2	1	2
3	3	2	3
2	2	1	2
1	3	1	1

Repeat Measures:

PL8AA	PLE8BB	IN8CC	INE8DD
2	2	2	3
3	3	3	2
3	3	3	3
3	3	2	2
3	2	1	2
3	3	2	2
3	2	1	3
3	3	3	3
3	3	2	2
3	3	3	2

PL161AA	PLE161BB	IN161CC	INE161DD
2	2	2	2
2	2	2	2
2	3	2	3
1	2	2	2
3	2	2	2
2	3	2	1
2	2	2	2
2	3	3	2
2	3	2	2
2	2	3	2

PL162AA	PLE162BB	IN162CC	INE162DD
2	2	1	2
2	3	1	2
3	3	2	3
2	2	2	2
2	2	1	3
3	3	1	2
2	2	1	2
3	3	1	2
2	2	1	2
2	2	1	2

Pt A

<u>PL8</u>

3	1	3	2
3	2	3	2
3	3	2	3
2	2	3	1
3	3	2	3
3	1	3	2
3	2	2	2
3	2	3	2
3	2	2	2
3	3	2	2

PLE8

3	3	2	3
2	3	2	3
3	3	2	3
2	2	3	3
3	3	1	3
3	2	3	3
3	3	2	2
3	3	2	3
2	2	2	2
3	3	3	3

IN8

3	3	3	3
2	2	2	2
3	3	3	3
2	3	2	1
2	2	3	3
2	2	3	2
3	3	3	2
2	2	2	2
3	2	3	3
2	3	3	2

INE8

2	2	2	1
3	3	2	2
2	2	1	2
2	2	3	2
2	2	1	2
3	2	3	3
1	2	1	1
2	2	2	3
2	2	2	2
2	3	3	2

PL161

2	2	3	3
3	2	3	3
3	3	3	3
2	2	3	3
3	3	3	3
2	3	3	3
3	3	3	3
3	3	3	3
2	3	3	3
3	3	3	3

PLE161

2	3	3	3
3	2	3	3
2	3	3	3
3	2	3	3
3	3	3	3
3	3	3	3
1	3	3	3
3	3	3	3
3	3	3	3
3	3	3	3

IN161

1	1	1	2
3	2	2	1
3	3	2	3
3	2	2	1
2	3	2	2
3	3	2	2
1	1	1	2
3	3	2	2
1	2	1	2
2	3	2	1

INE161

2	3	3	3
2	2	2	3
3	3	3	3
1	1	2	3
3	3	3	3
2	3	3	3
2	3	3	3
2	2	2	2
3	3	2	3
2	3	3	3

PL162

3	3	1	3
3	2	2	3
3	3	2	3
3	3	2	3
1	3	3	3
3	3	2	3
2	3	2	3
3	3	3	3
3	2	1	3
2	3	2	3

PLE162

2	3	3	3
3	3	3	3
3	3	3	3
3	3	3	2
3	3	3	3
3	2	3	3
2	3	3	3
3	3	3	3
3	3	3	3
3	3	3	3

IN162

3	2	2	1
2	2	1	2
2	3	3	2
2	1	1	2
3	3	2	2
2	3	1	3
3	2	2	2
1	2	2	3
1	1	3	1
3	3	1	3

INE162

2	3	3	2
3	2	2	2
2	2	2	3
3	3	3	2
1	3	3	1
3	3	3	3
1	1	2	1
2	3	3	2
2	2	2	2
2	3	3	3

Repeat Measures:

PL8AA	PLE8BB	IN8CC	INE8DD
3	3	2	3
3	2	3	2
3	3	2	3
2	3	2	3
3	2	2	3
3	3	3	3
3	3	1	2
3	3	3	3
2	3	2	1
3	3	1	2

PL161AA	PLE161BB	IN161CC	INE161DD
3	3	1	3
2	2	1	3
3	2	2	3
2	3	2	3
3	2	3	3
2	3	3	3
3	2	1	3
2	3	2	3
2	3	2	3
3	3	2	3

PL162AA	PLE162BB	IN162CC	INE162DD
3	3	1	2
3	3	3	2
3	3	1	2
3	3	2	1
2	3	2	3
3	3	2	3
2	2	1	3
3	3	3	3
2	3	1	3
2	3	3	2

Pt B

<u>PL8</u>

3	3	3	3
3	3	3	3
3	3	3	3
3	3	3	3
3	3	3	3
3	3	3	3
3	3	3	3
3	3	3	3
3	3	3	3
3	3	3	3

PLE8

3	3	3	3
3	3	3	3
3	3	3	3
3	3	3	3
3	3	2	3
3	3	3	3
3	3	2	3
3	3	3	3
3	3	3	3
3	3	3	3

IN8

3	3	3	3
3	3	2	2
3	3	3	3
3	3	1	2
2	2	3	3
3	3	3	2
3	3	3	2
3	2	2	3
3	3	3	3
3	3	3	2

INE8

3	2	3	2
3	3	3	3
3	3	3	3
3	3	3	3
3	3	3	3
3	3	3	3
2	3	3	3
3	3	3	3
2	3	3	3
3	3	3	3

PL161

3	3	3	3
3	3	3	3
3	3	3	3
3	3	3	3
3	3	3	3
3	3	3	3
3	3	3	3
3	3	3	3
3	3	3	3
3	3	3	3

PLE161

2	3	3	3
3	3	3	3
3	3	3	3
3	3	3	3
3	3	3	3
3	3	3	3
3	3	3	3
3	3	3	3
3	3	3	3
3	3	3	3

IN161

2	1	3	3
3	2	3	3
3	3	3	3
3	3	3	2
3	3	3	3
3	3	3	3
2	1	3	3
3	3	3	2
3	2	3	3
3	3	3	2

INE161

3	3	3	3
3	3	3	3
3	3	3	3
3	2	2	3
3	3	3	3
2	3	3	3
3	3	3	3
3	3	3	3
3	3	3	3
2	3	3	3

PL162

3	3	3	3
3	3	3	3
3	3	3	3
3	3	3	3
3	3	3	3
3	3	3	3
3	3	3	3
3	3	3	3
3	3	3	3
3	3	3	3

PLE162

3	3	3	3
3	3	3	3
3	3	3	3
3	3	3	3
3	3	3	3
3	3	3	3
3	3	3	3
3	3	3	3
3	3	3	3
3	3	3	3

IN162

3	3	3	1
3	3	3	3
3	3	3	3
3	1	2	3
3	3	3	3
3	2	3	3
3	3	3	3
3	3	3	3
2	3	3	2
3	1	1	3

INE162

2	3	3	3
3	3	3	3
2	3	2	3
3	3	3	3
3	3	3	3
3	3	3	3
3	3	3	3
3	3	3	3
3	3	3	3
3	3	3	3

Repeat Measures:

PL8AA	PLE8BB	IN8CC	INE8DD
3	3	3	3
3	3	3	3
3	3	3	3
2	3	2	3
3	3	3	3
3	3	3	3
3	3	3	3
3	3	3	3
3	3	2	3
3	3	3	3

PL161AA	PLE161BB	IN161CC	INE161DD
3	3	1	3
3	3	3	3
3	3	3	3
3	3	3	3
3	3	3	3
3	3	3	3
3	3	2	3
3	3	3	3
3	3	2	3
3	3	3	3

PL162AA	PLE162BB	IN162CC	INE162DD
3	3	3	3
3	3	3	3
3	3	2	3
3	3	3	3
3	3	3	3
3	3	3	3
3	3	2	3
3	3	3	3
3	3	3	3
3	3	3	3

Pogonion

<u>PL8</u>

3	3	3	3
3	3	3	3
3	3	3	3
3	3	3	3
3	3	3	3
3	3	3	3
3	3	3	3
3	3	3	3
3	3	3	3
3	3	3	3

PLE8

3	3	3	3
3	3	3	3
3	3	3	3
3	3	3	3
3	3	3	3
3	3	3	3
3	3	3	3
3	3	3	3
3	3	3	3
3	3	3	3

IN8

3	3	3	3
3	3	3	2
3	3	3	3
3	3	3	3
3	3	3	3
3	3	3	3
3	3	3	2
3	2	3	3
3	3	3	3
3	3	3	3

INE8

3	3	3	2
3	3	3	3
3	3	3	3
3	3	3	3
3	3	3	3
3	3	3	3
2	3	3	3
3	3	3	3
3	3	2	3
3	3	3	3

PL161

3	3	3	3
3	3	3	3
3	3	3	3
3	3	3	3
3	3	3	3
3	3	3	3
3	3	3	3
3	3	3	3
3	3	3	3
3	3	3	3

PLE161

3	3	3	3
3	3	3	3
3	3	3	3
3	3	3	3
3	3	3	3
3	3	3	3
3	3	3	3
3	3	3	3
3	3	3	3
3	3	3	3

IN161

2	2	3	3
3	3	3	3
3	3	3	3
3	3	3	3
3	3	3	3
3	3	3	3
2	2	3	3
3	3	3	3
3	3	3	3
3	3	3	2

<u>INE161</u>

3	3	3	3
3	3	3	3
3	3	3	3
3	3	3	3
3	3	3	3
3	3	3	3
3	3	3	3
3	3	3	3
3	3	3	3
3	3	3	3

<u>PL162</u>

3	3	3	3
3	3	3	3
3	3	3	3
3	3	3	3
3	3	3	3
3	3	3	3
3	3	3	3
3	3	3	3
3	3	3	3
3	3	3	3

<u>PLE162</u>

3	3	3	3
3	3	3	3
3	3	3	3
3	3	3	3
3	3	3	3
3	3	3	3
3	3	3	3
3	3	3	3
3	3	3	3
3	3	3	3

IN162

3	3	3	3
3	3	3	3
3	3	3	3
3	2	3	3
3	3	3	3
3	3	3	3
3	3	3	3
3	3	3	3
3	3	3	2
3	2	2	3

INE162

3	3	3	3
3	3	3	3
3	3	2	3
3	3	3	3
3	3	3	3
3	3	3	3
3	3	3	3
3	3	3	3
3	3	3	3
3	3	3	3

Repeat Measures:

PL8AA	PLE8BB	IN8CC	INE8DD
3	3	3	3
3	3	3	3
3	3	3	3
3	3	3	3
3	3	3	3
3	3	3	3
3	3	3	3
3	3	3	3
3	3	2	3
3	3	3	3

PL161AA	PLE161BB	IN161CC	INE161DD
3	3	2	3
3	3	3	3
3	3	3	3
3	3	3	3
3	3	3	3
3	3	3	3
3	3	3	3
3	3	3	3
3	3	3	3
3	3	3	3

PL162AA	PLE162BB	IN162CC	INE162DD
3	3	3	3
3	3	3	3
3	3	3	3
3	3	3	3
3	3	3	3
3	3	3	3
3	3	2	3
3	3	3	3
3	3	3	3
3	3	3	3

Pronasale

<u>PL8</u>

3	3	1	3
3	3	1	3
3	3	1	3
1	3	1	2
3	3	1	3
2	3	1	1
3	3	1	2
3	3	1	2
3	3	1	3
3	3	1	1

PLE8

3	3	3	3
3	3	3	3
3	3	2	3
3	3	1	3
3	3	2	3
3	3	3	3
2	3	2	3
3	3	3	3
3	3	3	3
3	3	3	3

IN8

1	3	3	3
2	2	3	3
2	3	3	3
1	1	3	3
2	3	3	3
1	1	1	3
2	3	2	2
1	3	2	2
2	2	3	3
1	3	2	3

INE8

2	2	2	3
3	3	3	3
2	2	2	3
2	3	3	3
2	2	1	3
3	3	3	3
2	3	2	3
2	3	3	3
3	2	3	3
3	3	3	3

PL161

1	1	1	1
1	1	1	1
1	1	1	1
1	1	1	1
1	1	3	1
1	1	1	1
1	1	1	1
1	1	1	1
1	1	1	1
1	1	1	1

PLE161

1	1	1	1
1	1	1	1
1	1	1	1
1	1	1	1
1	1	1	2
1	1	1	2
1	1	1	1
1	1	1	1
1	1	1	1
1	1	1	1

IN161

1	1	1	1
1	1	1	1
1	1	1	1
1	2	1	1
1	1	1	1
1	1	1	1
2	1	1	1
1	1	1	1
2	1	1	1
1	1	1	1

INE161

1	1	1	1
2	1	1	1
2	1	1	1
1	1	1	1
2	1	2	1
1	1	1	2
2	1	2	3
2	1	1	1
1	1	1	1
1	1	2	1

PL162

1	1	2	1
1	1	2	2
1	3	2	3
3	1	2	2
1	1	1	2
2	1	2	2
1	2	2	2
3	1	1	2
2	1	2	2
1	1	1	1

PLE162

1	2	2	3
2	3	2	3
3	3	3	3
2	3	2	2
2	3	2	3
1	2	1	2
2	3	2	3
1	3	2	2
2	2	2	3
1	2	1	2

IN162

3	3	3	3
3	2	3	3
2	3	3	3
2	1	3	3
3	2	2	3
3	2	3	3
3	2	2	3
3	2	3	3
3	3	3	3
3	2	2	3

INE162

2	3	2	3
3	3	2	3
2	3	2	2
2	3	2	3
2	3	2	2
3	3	3	3
1	2	2	2
3	3	3	3
3	3	3	3
2	3	3	3

Repeated Measures:

PL8AA	PLE8BB	IN8CC	INE8DD
2	3	2	3
3	3	3	3
1	3	2	3
1	3	3	3
3	3	2	3
1	3	3	3
3	3	1	3
2	3	3	3
2	3	3	3
2	3	3	3

PL161AA	PLE161BB	IN161CC	INE161DD
1	1	1	1
1	1	1	1
1	1	1	1
1	1	1	1
1	1	1	2
1	1	1	1
1	1	1	1
1	1	1	1
1	1	1	1
1	1	1	1

PL162AA	PLE162BB	IN162CC	INE162DD
1	2	1	3
1	3	3	3
1	2	3	3
2	2	2	3
1	2	2	3
2	3	3	3
1	2	3	2
3	3	3	2
1	3	3	3
1	2	2	3

Labrale Superius

<u>PL8</u>

3	3	2	1
2	3	2	2
3	3	2	3
1	3	1	1
3	3	1	2
3	3	2	1
2	3	1	2
3	3	3	1
3	3	2	2
3	3	1	1

PLE8

1	2	3	2
2	3	3	2
3	3	3	2
3	3	2	3
2	3	2	2
2	3	3	2
2	3	3	2
3	3	3	3
2	3	2	2
3	3	3	1

IN8

3	3	3	3
2	2	2	2
3	2	3	3
1	2	2	2
2	3	3	3
2	2	2	2
3	3	2	2
3	3	3	3
3	3	3	3
3	3	2	2

INE8

2	3	2	2
2	3	3	2
2	3	2	2
2	3	3	3
1	2	3	2
3	3	3	3
1	3	2	2
2	3	3	3
2	2	2	2
2	3	3	3

PL161

3	1	1	1
3	1	1	2
3	1	3	2
3	1	1	1
3	1	3	2
3	1	2	1
3	1	2	2
3	1	2	1
3	1	1	2
3	1	2	1

PLE161

1	1	1	1
1	1	1	2
2	3	3	3
1	1	1	2
1	2	3	2
2	1	1	1
1	1	1	2
2	2	2	2
2	2	2	2
1	1	2	2

IN161

3	3	3	2
3	3	3	2
3	2	3	3
2	2	1	3
1	2	1	3
3	3	3	1
2	1	1	2
2	3	2	3
3	2	2	3
2	1	2	3

INE161

1	1	2	2
3	2	2	2
3	3	3	2
1	1	1	2
3	2	3	2
1	1	1	2
3	1	1	2
2	2	2	3
2	1	2	2
2	2	3	2

PL162

2	1	2	2
1	2	3	2
2	3	3	3
3	1	2	2
1	2	2	3
3	1	3	2
1	2	3	3
3	2	3	3
2	2	3	3
1	1	2	3

PLE162

2	3	2	3
2	3	2	3
3	3	3	3
2	3	3	3
2	3	3	3
2	3	1	3
2	3	2	3
2	3	2	3
2	2	3	3
2	2	3	3

IN162

3	3	3	3
3	3	3	3
2	3	3	3
2	3	3	3
3	3	3	3
3	2	3	3
3	3	2	3
3	2	3	3
3	3	3	3
3	3	3	3

INE162

3	3	3	3
3	3	3	3
2	3	2	3
2	3	2	3
2	3	2	3
3	3	3	3
2	2	2	3
3	3	3	3
3	3	3	3
3	3	3	3

Repeated Measures:

PL8AA	PLE8BB	IN8CC	INE8DD
2	3	3	2
2	3	3	3
3	3	3	3
1	3	2	2
3	3	3	3
3	3	3	3
3	3	2	2
3	3	3	3
3	3	2	3
3	3	3	3

PL161AA	PLE161BB	IN161CC	INE161DD
1	1	2	1
2	1	3	2
2	1	3	3
1	2	2	2
3	1	1	2
1	2	3	2
1	1	1	2
2	3	3	2
1	2	2	2
1	1	3	1

PL162AA	PLE162BB	IN162CC	INE162DD
2	2	1	3
2	3	3	3
2	3	3	3
2	2	2	3
2	3	3	3
2	3	3	3
1	2	3	2
3	3	3	3
2	3	3	3
1	3	3	3

Labrale Inferius

<u>PL8</u>

3	3	2	1
3	3	2	2
3	3	2	3
2	3	1	1
3	3	1	2
3	3	2	1
2	3	1	2
3	3	3	1
2	3	2	2
3	3	1	1

PLE8

1	2	2	2
2	3	3	2
3	3	3	2
2	2	2	3
2	3	2	2
2	3	3	2
3	3	2	2
3	2	3	3
2	3	2	2
2	3	3	1

IN8

3	3	3	3
2	2	2	2
3	2	3	3
2	3	2	2
3	3	3	3
2	2	2	2
3	3	2	2
3	3	3	3
2	3	3	3
3	3	2	2

INE8

2	3	2	2
2	3	3	2
2	3	2	2
2	3	3	3
1	2	3	2
3	3	3	3
1	3	2	2
3	3	3	3
2	3	2	2
2	3	3	3

PL161

3	1	1	1
3	1	1	2
3	2	3	3
3	1	1	1
3	1	3	2
3	1	2	1
3	1	2	2
3	1	2	2
3	1	1	2
3	1	2	1

PLE161

1	1	1	1
1	1	2	3
2	3	3	3
1	2	1	2
1	2	3	3
2	1	1	1
1	1	1	2
3	2	2	2
2	2	2	2
1	1	2	2

IN161

3	3	3	2
3	3	3	2
3	2	3	3
2	2	1	3
1	2	1	3
3	3	3	1
2	1	3	2
2	3	3	3
3	2	2	3
3	1	2	3

INE161

1	1	2	2
3	2	2	2
3	3	3	2
2	1	1	2
3	2	3	2
1	1	1	3
3	1	1	3
2	2	2	3
2	2	2	2
2	2	3	3

PL162

2	1	2	2
2	2	3	3
2	3	3	3
3	1	2	3
1	2	2	3
3	1	3	3
1	2	3	3
3	2	3	3
2	2	3	3
1	1	2	3

PLE162

2	1	2	2
2	2	3	3
2	3	3	3
3	1	2	3
1	2	2	3
3	1	3	3
1	2	3	3
3	2	3	3
2	2	3	3
1	1	2	3

IN162

3	3	3	3
3	3	3	3
2	3	3	3
2	3	3	3
3	3	3	3
3	2	3	3
3	3	2	3
3	2	3	3
3	3	3	3
3	3	3	3

INE162

3	3	3	3
3	3	3	3
2	3	2	3
2	3	2	3
2	3	2	3
3	3	3	3
2	2	2	3
3	3	3	3
3	3	3	3
3	3	3	3

Repeated Measures:

PL8AA	PLE8BB	IN8CC	INE8DD
2	2	2	2
2	3	3	3
3	3	3	3
1	3	2	2
3	3	3	3
3	2	3	3
3	2	2	2
3	3	3	3
3	3	2	3
3	2	3	3

PL161AA	PLE161BB	IN161CC	INE161DD
1	1	2	2
2	1	3	3
3	1	3	3
1	2	2	2
3	1	1	2
1	3	3	2
1	1	2	2
2	3	3	2
1	2	2	2
1	1	3	2

PL162AA	PLE162BB	IN162CC	INE162DD
2	2	1	3
3	3	3	3
2	3	3	3
2	2	2	3
2	3	3	3
2	3	3	3
1	2	3	2
3	3	3	3
2	3	3	3
1	3	3	3

Soft Tissue Pogonion

<u>PL8</u>

3	3	3	1
3	3	3	2
3	3	2	3
2	3	2	1
3	3	2	2
3	2	2	1
3	3	2	2
3	3	3	2
3	3	3	2
3	3	1	1

PLE8

1	2	2	2
2	2	2	2
3	3	3	3
3	2	2	3
2	2	2	2
2	2	3	2
2	3	2	3
3	2	3	3
2	3	2	2
3	3	2	1

IN8

3	3	3	3
3	3	2	3
3	2	3	3
2	1	3	3
3	3	3	3
2	2	2	2
3	3	2	2
3	3	3	3
3	3	3	3
3	3	2	3

INE8

2	3	2	2
3	3	3	3
3	3	2	3
2	3	3	3
2	2	2	2
3	3	3	3
2	3	2	3
3	3	3	3
3	3	2	3
3	3	3	3

PL161

3	1	2	2
3	1	3	3
3	2	3	3
3	1	3	2
3	1	3	2
3	1	3	2
3	1	3	2
3	1	3	2
3	1	2	3
3	1	3	3

PLE161

2	1	1	2
1	2	3	2
2	3	3	3
1	2	2	2
2	2	3	3
2	1	2	2
1	2	2	2
3	3	3	2
2	2	3	2
2	2	2	2

IN161

3	3	3	3
3	3	3	3
3	2	3	3
2	2	2	3
2	3	2	3
3	3	3	2
2	2	3	2
2	3	3	3
3	3	3	3
3	3	3	3

INE161

3	2	2	2
3	2	3	2
3	3	3	2
2	2	3	2
3	2	3	2
2	2	2	3
3	2	3	3
3	2	3	3
3	2	2	3
2	2	3	3

PL162

3	1	1	2
2	2	3	3
2	3	3	3
3	1	2	3
2	2	2	3
3	2	3	3
2	2	3	3
3	2	3	3
3	2	3	3
1	1	3	3

PLE162

2	3	2	3
2	3	2	3
3	3	3	3
2	3	3	3
2	3	2	3
2	3	2	3
2	3	2	3
2	3	3	3
2	3	2	3
2	3	3	3

IN162

3	3	3	3
3	3	3	3
2	3	3	3
2	3	3	3
3	3	3	3
3	2	3	3
3	3	2	3
3	2	3	3
3	3	3	3
3	3	3	3

INE162

2	3	3	3
3	3	3	3
2	3	2	3
2	3	2	3
2	3	2	3
3	3	3	3
2	2	3	3
3	3	3	3
2	3	3	3
3	3	3	3

Repeated Measures:

PL8AA	PLE8BB	IN8CC	INE8DD
3	2	2	3
3	3	2	3
3	3	3	3
2	3	2	2
3	2	2	3
3	2	3	3
3	2	3	3
3	3	3	3
3	2	2	3
3	2	3	3

PL161AA	PLE161BB	IN161CC	INE161DD
2	3	2	2
3	1	3	3
3	1	3	3
2	2	2	2
3	2	2	2
2	3	3	2
2	2	3	2
2	3	3	2
3	2	3	2
2	2	3	2

PL162AA	PLE162BB	IN162CC	INE162DD
2	3	1	3
3	3	3	3
2	3	3	3
2	2	2	3
1	3	3	3
3	3	3	3
1	3	3	2
3	3	3	3
2	3	3	3
1	3	3	3

Overall Image

<u>PL8</u>

3	1	2	1
3	1	1	2
3	1	2	2
2	1	1	1
3	2	2	2
3	2	2	2
3	2	1	2
3	2	2	2
3	1	1	2
3	2	1	1

PLE8

2	2	2	2
2	2	2	2
3	3	2	3
3	1	2	3
3	3	2	2
2	2	2	2
2	2	2	2
3	2	3	3
3	3	2	2
3	3	2	2

IN8

3	2	3	2
1	2	1	1
2	2	3	2
1	2	1	1
2	2	3	2
2	1	2	2
3	2	2	2
2	1	2	2
3	3	3	2
2	3	2	2

INE8

1	3	3	1
2	3	3	2
2	2	2	2
2	3	3	3
2	2	2	2
2	3	2	2
1	3	2	1
2	3	3	3
2	3	1	2
2	3	3	2

PL161

2	1	1	1
2	1	1	1
2	1	2	1
1	1	1	1
2	1	2	2
2	2	2	2
2	1	2	1
2	1	2	2
1	1	1	1
3	1	3	1

PLE161

1	1	1	1
1	1	1	1
2	2	2	1
1	2	1	2
2	2	2	2
2	2	2	2
1	1	1	2
1	2	2	2
1	2	2	1
1	2	2	2

IN161

1	1	2	1
1	1	1	1
2	2	2	1
2	2	1	1
2	2	2	2
2	2	2	2
1	1	1	2
1	2	1	2
1	1	1	1
1	1	2	1

INE161

2	2	3	2
2	1	1	1
2	2	2	2
1	1	1	1
2	2	2	2
2	2	2	2
3	1	2	2
2	2	2	2
1	1	2	2
1	2	3	2

PL162

2	1	1	1
1	1	1	1
2	2	2	2
2	1	2	2
1	2	2	2
2	2	2	2
1	2	1	2
2	2	2	2
1	2	1	2
1	1	1	2

PLE162

1	3	2	1
1	2	1	2
2	2	2	2
1	3	2	1
2	3	2	3
2	1	2	2
2	3	2	2
2	2	2	2
2	2	2	2
2	2	2	2

<u>IN162</u>

1	2	1	1
2	2	1	2
2	2	2	2
2	1	1	3
2	2	2	2
1	2	2	3
2	2	2	2
1	2	2	2
2	1	1	1
2	1	3	2

<u>INE162</u>

2	3	2	2
1	3	2	2
2	3	2	2
2	3	2	2
2	3	2	2
2	3	2	3
2	2	1	2
2	3	2	3
1	2	1	2
1	3	2	1

Repeated Measures:

PL8AA	PLE8BB	IN8CC	INE8DD
2	2	2	3
2	3	2	3
2	3	2	3
1	3	2	2
3	2	2	3
3	2	2	3
3	2	1	2
3	3	2	2
3	2	2	1
3	2	2	3

PL161AA	PLE161BB	IN161CC	INE161DD
1	3	1	2
1	1	1	2
2	2	2	2
1	2	2	1
2	2	2	2
2	2	2	1
1	1	1	1
2	2	1	2
1	1	1	1
2	1	2	1

PL162AA	PLE162BB	IN162CC	INE162DD
2	2	1	3
2	3	1	2
2	3	2	2
2	2	2	2
2	3	2	3
2	3	2	3
2	2	1	2
3	2	2	2
1	2	1	2
1	2	2	2

CURRICULUM VITAE

NAME: Ryan B. Wiesemann

ADDRESS: University of Louisville School of Dentistry

DOB: Lexington, Kentucky – May 16, 1977

EDUCATION
& TRAINING: B.B.A, Finance & Entrepreneurship
       Emory University
       1995-99

       D.M.D., Dentistry
       University of Louisville School of Dentistry
       2000-04

PROFESSIONAL SOCIETIES:

       American Dental Association
       Kentucky Dental Association
       International Academy of Sports Dentistry
       Psi Omega Dental fraternity
       Kentucky Student Dental Association

PUBLICATIONS:
       Pseudo-Color and Emboss Enhancements in Photostimulable
       Phosphor Cephalometrics. R. WIESEMANN*, K. WEST, D.
       TASMAN, A. SILVEIRA, J.SCHEETZ, B. JOHNSON, T.
       FARMAN, A. FARMAN (ULSD, KY, USA), Int Assoc Dent Res,
       San Antonio, TX. *J Dent Res*   2003 (Abstr 0307).